A Double-edged Sword: Evolutionary Novelty along Deep-time Diversity Oscillation in An Iconic Group of Predatory Insects (Neuroptera: Mantispoidea)

HONGYU LI[1], DE ZHUO[2], BO WANG[3], HIROSHI NAKAMINE[4], SHÛHEI YAMAMOTO[5], WEIWEI ZHANG[6], JAMES E. JEPSON[7], MICHAEL OHL[8], ULRIKE ASPÖCK[9, 10], HORST ASPÖCK[11], THET TIN NYUNT[12], MICHAEL S. ENGEL[13], MICHAEL J. BENTON[14], PHILIP DONOGHUE[14], AND XINGYUE LIU[1,15]*

[1]Department of Entomology, China Agricultural University, Beijing 100193, China;
[2]Beijing Xiachong Amber Museum, 9 Shuanghe Middle Road, Beijing 101399, China;
[3]State Key Laboratory of Palaeobiology and Stratigraphy, Nanjing Institute of Geology and Palaeontology, Chinese Academy of Sciences, Nanjing 210008, China;
[4]Minoh Park Insect Museum, Minoh Park 1–18, Minoh City, Osaka 562-0002, Japan;
[5]Hokkaido University Museum, Hokkaido University, Sapporo 060-0810, Japan;
[6]Three Gorges Entomological Museum, Chongqing 400015, China;
[7]Department of Earth and Environmental Sciences, University of Manchester, Manchester M13 9PL, UK;
[8]Museum für Naturkunde, Berlin 10115, Germany;
[9]Naturhistorisches Museum Wien, Zweite Zoologische Abteilung, Burgring 7, A-1010, Vienna, Austria;
[10]Department of Evolutionary Biology, University of Vienna, Althanstraße 14, A-1090, Vienna, Austria;
[11]Institute of Specific Prophylaxis and Tropical Medicine, Medical Parasitology, Medical University of Vienna, Kinderspitalgasse 15, A-1090, Vienna, Austria;
[12]Department of Geological Survey and Mineral Exploration, Ministry of Natural Resources and Environmental Conservation, Myanmar Gems Museum, Nay Pyi Taw 15011, Myanmar;
[13]Division of Invertebrate Zoology, American Museum of Natural History, 200 Central Park West, New York, New York 10024-5192, USA;
[14]Bristol Palaeobiology Group, School of Earth Sciences, University of Bristol, Bristol BS8 1RJ, UK;
[15]Institute of Zoology, Chinese Academy of Sciences, Beijing 100101, China.
** Correspondence to be sent to: Department of Entomology, China Agricultural University, Beijing 100193, China*
E-mail: liuxingyue@cau.edu.cn

Running Title: Novelties and Diversification of Mantispoidea

Abstract.—Evolutionary novelties are commonly identified as drivers of lineage diversification, with key innovations potentially triggering adaptive radiation. Nevertheless, testing hypotheses on the role of evolutionary novelties in promoting diversification through deep time has proven challenging. Here we unravel the role of the raptorial appendages, with evolutionary novelties for predation, in the macroevolution of a predatory insect lineage, the Superfamily Mantispoidea (mantidflies, beaded lacewings, thorny lacewings, and dipteromantispids), based on a new dated phylogeny and quantitative evolutionary analyses on modern and fossil species. We demonstrate a

single origin of the raptorial foreleg and its associated novelties as key innovations triggering an early radiation of raptorial mantispoids from the Late Triassic to the Early Jurassic. Subsequently, the evolution of the raptorial foreleg influenced the diversification in different modes among lineages. At times, it might have limited the morphological diversity of other body parts and lead to lineage constraint by intensifying competition and lowering environmental resilience, e.g., in thorny lacewings, whose extant diversity is meagre. Conversely, in mantidflies, reduced emphasis on foreleg novelties and increased plasticity in other body parts may lead to better adaptation to predator-prey interactions and environmental shifts, thus maintaining a stable or accelerated level of diversification. We also reveal how major environmental change and lineage interactions interplayed with raptorial novelties in shaping the significant oscillations of mantispoid diversification over deep time, especially the abrupt shift near the mid-Cretaceous. However, by excluding a substantial portion of samples from the mid-Cretaceous of Myanmar, these shifts of some evolutionary parameters, such as morphological disparity, body size, and diversification rates, became inconspicuous and might be overestimated due to sampling bias. Our results uncover the intricate evolutionary patterns and profound significance of raptorial specializations, providing new insights into the role of novelties in forming evolutionary trajectories, both for the better and worse. [evolutionary novelty; macroevolution; diversification; raptorial foreleg; fossil; insect; Mantispoidea]

INTRODUCTION

Evolutionary novelties are a prominent theme in explaining the diversification of lineages (Heard and Hauser 1995, Hunter 1998, Erwin 2015). Some studies noted that evolutionary novelties may emerge without achieving notable ecological or evolutionary success, and unnecessarily trigger diversification. However, some distinct novelties do also exist and have a positive ecological impact on the evolution of lineages, being defined as the innovations (Hunter 1998, Erwin 2015, Rabosky 2017). Among them, key innovations may enable lineages to reach previously inaccessible ecological states, such as in exploiting new or underutilized resources, colonizing new niches, promoting fitness, or avoiding predation, which are invoked liberally within evolutionary biology as triggers of adaptive radiation (Gianoli 2004, Roquet et al. 2013, Benson et al. 2014, Nicholson et al. 2014, Erwin 2015, Hull 2015, Condamine et al. 2016, Stroud and Losos 2016, Marki et al. 2019, Blaimer et al. 2023, Miller et al. 2023). However, testing the impact of evolutionary novelties and the hypotheses of key innovations across time have proven challenging. In large part, this is because many such events have taken place particularly deep in the time-scale of evolution, leaving few molecular and palaeontological evidence available to trace phenotypic evolution and lineage diversification (Gould and Eldredge 1977, Vermeij 2001, Benton and Donoghue 2007, Donoghue and Benton 2007, Lloyd et al. 2012, Erwin 2015, Rabosky 2017). Besides, there has also been limited methods for testing the hypotheses of evolutionary novelty (Erwin 2015).

Arthropods, well-known for their vast diversity and evolutionary longevity, exhibit a plethora of phenotypic novelties that can serve as a basis for testing hypotheses on the relationship between the evolution of novelties and their relative ecological or evolutionary impact. Raptorial appendages have often been claimed as innovations for predation, which have evolved multiple times independently from homologous or nonhomologous appendages (e.g., chelicerae, pedipalps, maxillipeds and forelegs) among diverse arthropod groups including radiodonts, amblypygids,

spiders, scorpions, crustaceans, insects, etc. (Aspöck et al. 1980a, Aspöck et al. 1980b, Anker et al. 2006, Vannier et al. 2009, Porter et al. 2010, Kral 2013, Lamsdell et al. 2013, Wieland 2013, Castro-Huertas et al. 2019, Lu et al. 2020, Oufiero 2020, Moysiuk and Caron 2021, Schmidt et al. 2022). Raptorial appendages are usually characterized by elongate, strengthened, and flattened limbs with sharp spines. They have been identified as a fundamental trait driving the predator-prey arms race in the Cambrian radiation of bilaterian animals (Lamsdell et al. 2013, Sperling et al. 2013, Lerosey-Aubril and Pates 2018, Moysiuk and Caron 2021), representing a successful adaptation of arthropod predators to the challenges of hunting, feeding and protection across diverse ecological niches. Although previous studies have alluded to the potential of raptorial appendages as key innovations driving lineage diversification, comprehensive and robust validation of this hypothesis is still lacking (Lu et al. 2020, Moysiuk and Caron 2021, Lai et al. 2023).

In this context, we have directed our research towards the evolution of raptorial forelegs in an iconic predatory group of insects as a test case to shed light on understanding the manifestations of evolutionary novelties in deep time. These insects, classified under the Superfamily Mantispoidea, comprise a part of Neuroptera—a key holometabolous order with an evolutionary history of over 300 million years, a large number of archaic morphological and biological traits, and rich fossil records and relict extant species, shedding profound insights into insect evolution (Grimaldi et al. 2002, Lu and Liu 2021). Mantispoidea showcases a diversity of foreleg phenotypic variety, including both cursorial and diverse raptorial forelegs, including transitional and highly specialized forms (Lu et al. 2020, Nakamine et al. 2020, Li et al. 2022, Li et al. 2023). The mantispoid raptorial appendages adhere to the typical subchelate model: the prehensile leg (foreleg) incorporates an enlarged propodite (profemur), while the dactylopodite (protibia) is recurved against the ventral surface of the propodite, further complemented with integumentary specializations and thickened setae (Poivre 1974, Poivre 1978, Weirauch et al. 2011, Wieland 2013, Pérez-de la Fuente and Peñalver 2019, Ardila-Camacho et al. 2021). This superfamily is currently classified into Berothidae (beaded lacewings), and three raptorial families (raptorial Mantispoidea or Raptoneuroptera), i.e., Rhachiberothidae (thorny lacewings), †Dipteromantispidae (recorded only from the Cretaceous), and Mantispidae (mantid lacewings or mantidflies). It encompasses about 530 species in 74 genera in the modern global fauna, and 165 species in 106 genera among extinct forms (Supplementary Table S1), with an evolutionary history spanning over 200 million years (Makarkin et al. 2011, Engel et al. 2018, Li et al. 2020, Lu et al. 2020, Ardila-Camacho et al. 2021, Lu and Liu 2021, Oswald 2022, Khramov 2023, Li et al. 2023). Considering these attributes, Mantispoidea represents an ideal model for probing the intricacies of raptorial appendage evolution in arthropod predators, offering a window into the investigation of evolutionary novelties on a deep timescale.

We undertook a novel morphology-based phylogenetic analysis of Mantispoidea incorporating comprehensive samples of living and fossil lineages across the evolutionary history. A tip-dating approach was used to infer the temporal scale of lineage divergences. Based on the new time-tree of Mantispoidea, we elucidated the evolutionary dynamics of phenotypic rates and disparity, and assessed the interplay between morphological evolution and lineage diversification using quantitative paleobiological methods, considering a role for both biotic and abiotic factors. Moreover, we conducted a quantitative study on the impact of intra- and inter-clade interactions on diversification. Our results support the hypothesis that raptorial foreleg novelties served as key

innovations triggering an early adaptive radiation of mantispoids from the Late Triassic to the Early Jurassic. However, the impact of later raptorial foreleg novelties on lineage diversification throughout evolutionary history was not always positive. In some lineages, these novelties appear to have constrained their evolution, leading to ecological specialization and even to the demise of some lineages in tandem with environmental change. Additionally, the broader Mesozoic environmental shifts and complex intra- and inter-clade interactions further compounded the evolutionary dynamics. Our study sheds light on the impact of the raptorial lifestyle on diversification from the perspective of macroevolution, offering valuable insights into how novelties shape the evolutionary trajectory over deep timescales.

MATERIALS AND METHODS

To simplify the understanding of the numerous methods and complex workflow in this study, we have summarized the process in a pipeline, as shown in Fig. 1.

Material and Sampling

Sampling for the phylogenetic analysis included a wide range of taxa across all families and subfamilies of extant and extinct Mantispoidea. For the extant taxa, 131 specimens of 26 genera and 43 species of Berothidae, Mantispidae, Osmylidae, and Dilaridae (the latter two families are outgroup taxa) were examined. For the extinct taxa, we studied 129 amber specimens from the Hukawng Valley in Tanai Township, Myitkyina District of Kachin State, Myanmar (Kania et al. 2015), which covers four mantispoid families, 34 genera and 66 species. The age of the amber deposit has been investigated and dated to be 98.8 ± 0.6 million years by U-Pb dating of zircons from the volcanoclastic matrix of the amber (Shi et al. 2012). Additionally, we examined 75 high-definition photographs of six genera and nine species of †Mesomantispinae (compressed fossils, as well as the type specimens of †*Mantispidiptera enigmatica* Grimaldi and †*Jersimantispa henryi* (Grimaldi) from New Jersey amber (see specimen locations in Supplementary Appendix 1).

We initially sampled 143 mantispoid ingroup taxa (most at generic level, some at species level) including 14 subfamilies and four families, ensuring the sampling was as adequate as possible for representative lineages and morphotypes. We subsequently removed three genera with dubious familial placement (i.e., †*Nascimberotha*, †*Liassochrysa* and †*Promantispa*, see Supplementary Appendix 4), and further removed all fossil taxa that are fragmentarily preserved or with only isolated wings described, as this leads to a high proportion of missing data (i.e., †*Berothone*, †*Caririberotha*, †*Epimesoberotha*, †*Khasurtoberotha*, †*Krokhathone*, †*Mesithone*, †*Mesomantispa*, †*Prosagittalata*, †*Symphrasites*, †*Vectispa* and †*Gerstaeckerella asiatica*). Thus, three morphomatrices with different sampling strategies were established to explore the impact of the above taxa in phylogenetic inference. *Osmylus* (Osmylidae), *Dilar montanus* and †*D. cretaceous* (Dilaridae) were sampled as outgroup taxa (Liu et al. 2015, Wang et al. 2017, Winterton et al. 2018, Lu et al. 2020).

In summary, the present fossil samples used for analyses came from various deposits globally: six from Lebanese amber (130–125.5 Ma); four from Spanish amber (112–99.6 Ma); one from Charentese amber, France (105.3–99.6 Ma); 49 from Kachin amber, Myanmar (99.6–93.5 Ma); seven from New Jersey amber, USA (93.9–89.8 Ma); one from Kuji amber, Japan (89.3–83.5 Ma); one from Hat Creek amber, Canada (56–47.8 Ma); one from Grassy Lake amber, Canada (83.5–70.6 Ma); one from Oise amber, France (56–47.8 Ma); four from Baltic amber (38–33.9 Ma); two from Dominican

amber (20.4–13.8 Ma); one from Dobbertin, Germany (183–182 Ma); five from Daohugou, China (166.1–157.3Ma); 14 from Karatau, Kazakhstan (166.1–157.3 Ma); one from Purbeck Limestone Group, England (145–140.2 Ma); six from Huangbanjigou (130–125.5 Ma), China; one from Ryonsang-dong, North Korea (129.4–113 Ma); four from Baissa, Russia (125–113 Ma); two from Crato Formation, Brazil (122.5–112 Ma); one from Kzyl-Zhar, Kazakhstan (93.9–89.8 Ma); one from Gus' Pit, USA (56–47.8 Ma); one from Grube Messel, Germany (48.6–40.4 Ma); one from UCM locality 2009063, Garfield County, USA (46.2–40.4 Ma); one from Bembridge, UK (38–33.9 Ma); and one from Céreste, France (33.9–38.4 Ma).

Morphological Dataset

We coded 232 discrete adult characters on head, thorax, legs, wings and genitalia (see Supplementary Appendix 3), based on direct examinations of specimens and previously published data (Lambkin 1986b, Lambkin 1986a, Willmann 1990, Aspöck and Mansell 1994, Aspöck and Nemeschkal 1997, Aspöck and Randolf 2014, Liu et al. 2015, Lu et al. 2020, Ardila-Camacho et al. 2021). There are 16 autapomorphic characters in our datasets, which are parsimony-uninformative but directly impact on branch length estimates and evolutionary rates (Matzke and Irmis 2018, Gavryushkina and Zhang 2020, Simoes et al. 2020a). The matrix was constructed on Mesquite v. 3.6. Inapplicable and unknown characters were coded as "-" and "?", respectively. We use "&" and "/" to connect different character states respectively of polymorphic and uncertain data. Three matrices were created: matrix 146T (232×146 taxa), matrix 132T (232×132 taxa) and matrix 143T (232×143 taxa).

Phylogenetic Analyses

We reconstructed the phylogeny based on the aforementioned three morphological matrices by using three approaches of phylogenetic inference. Maximum parsimony analyses (MP) were conducted in TNT v. 1.5 (Goloboff and Catalano 2016) with all characters non-additive, unordered, and under equal weights (EW). All heuristic searches were performed using the initial traditional search (T), with starting trees with random seed=1, 1000 replications, Tree Bisection Reconnection (TBR) branch swapping, and holding 10 trees per replication. The additional new technology search (N) was also carried out with sectorial search, ratchet, tree drift, and tree fuse options with default parameters. Bremer support values and Bootstrap values were calculated with the function implemented in TNT (Setting for Bremer support values calculation: TBR from existing trees, retain trees suboptimal by 100 steps; setting for Bootstrap values calculation: traditional search, number of replicates: 1000). Homoplasious and homologous character states output by TNT were illustrated on the strict consensus tree using Adobe Illustrator CC2021. The results were abbreviated as MP1T/N (146×232), MP2T/N (132×232) and MP3T/N (143×232) respectively (Supplementary Figs. S3a, S4a, S5a, S60).

Maximum likelihood analyses (ML) were performed using IQ-TREE v. 1.6.12 (Nguyen et al. 2015). ModelFinder, the built-in program for automatic model selection in IQ-TREE (Kalyaanamoorthy et al. 2017), sometimes selected "MK+FQ+ASC+R3" (R3) and other times "MK+FQ+ASC+G4" (G4) as the best-fit model for different datasets, indicating potential instability in the automatic model selection process. Therefore, to control the variables and determine the impact of both the unstable model selection and datasets on phylogeny, we performed separate analyses for each dataset under both models. The branch support values were

estimated by 1000 ultrafast bootstraps. To obtain more stable tree topology, ten independent runs were executed and the result with the largest likelihood was selected as the best ML tree (Yin et al. 2021). The results were abbreviated as ML1R/G (146×232), ML2R/G (132×232) and ML3R/G (143×232) respectively (Supplementary Figs. S3b, S4b, S5b, S61).

Bayesian inference (BI) was performed using MrBayes v. 3.2.7a (Ronquist et al. 2012). The unordered Mkv model (variable coding) were utilized to analyse the morphological character evolution for our dataset (Lewis 2001, Ronquist et al. 2012, Simoes et al. 2020a). We evaluated the best-fitting probability mass functions (gamma or lognormal) to model among character rate variation, using only the 143×232 dataset as a representative for computational efficiency. This was done using the stepping-stone sampling strategy to assess the marginal model likelihoods (Xie et al. 2011) and calculating Bayes factors (BF) (Kass and Raftery 1995, Nylander et al. 2004) over 50 steps for 700 million generations. Given the anomalous marginal likelihood value (35713.09) appeared in the fourth run of the evaluation with lognormal model, we only focused on the first three runs. Our findings indicated that the gamma model (-6074.04) fits our dataset better than lognormal model (-6462.93), with a BF of $2\ln(B_{10}) = 777.78$. Moreover, we opted for the gamma distribution, as it is more commonly used, thereby facilitating comparison with previous studies. Searches were run for 40 million generations with four runs, six chains of five heated and one cold, and 50% of sampled trees as burn-in were removed. The maximum compatibility tree (MCT, contype=allcompat) were output. The convergence and mixing of the MCMC chains were evaluated in Tracer v1.7.2 (Rambaut et al. 2018) and R package "convenience" (Fabreti and Hoehna 2022), to ensure the multiple runs converged on the same distribution and ascertain that effective sample sizes (ESS) exceeding 200. The results were abbreviated as BI1 (146×232), BI2 (132×232) and BI3 (143×232) respectively (Supplementary Figs. S3c, S4c, S5c; see more detailed settings on Dryad at https://doi.org/10.5061/dryad.h18931zth).

Divergence Time and Evolutionary Rate Estimations

The morphological matrix excluding three dubious taxa (143×232) was selected for divergence time and evolutionary rate estimations, which contains comparatively convincing and sufficient taxonomic and fossil information. The divergence time and evolutionary rate were estimated by tip-dating analysis with the relaxed morphological clocks and the skyline fossilized birth-death tree model (SFBD) using MrBayes 3.2.7a (Gavryushkina et al. 2014, Zhang et al. 2016, Simoes et al. 2020a). To detect the best fitting clock model and rate prior, we performed Bayes factors (BFs) applying model fitting analysis using the stepping-stone sampling strategy (Xie et al. 2011) to assess the marginal model likelihoods for the uncorrelated (independent gamma rate (IGR) (Lepage et al. 2007)) and autocorrelated clock models (continuous autocorrelated clock of Thorne and Kishino (TK02) (Thorne and Kishino 2002)) respectively under the gamma and lognormal distributions for the base of clock rate for the matrix, setting 50 steps for 800 million generations. Four different clock model combinations were generated: IGR+ga, IGR+ln, TK02+ga and TK02+ln. The resulting marginal model likelihoods are respectively: -4890.89, -4005.16, -4932.77 and -4926.40. Therefore, the IGR+ln model has a higher marginal likelihood than all other models, with a BF of $2\ln(B_{10}) = 1771.46$ relative to the second best-ranking model (IGR+ga). This is a significant difference between models and indicates a very strong preference for the IGR+ln model (Kass and Raftery 1995, Nylander et al. 2004).

Considering the debates on incorporating stratigraphic data into phylogenetic analysis (Fisher 2008, King et al. 2017, Turner et al. 2017, King 2021) and the inconsistence of tree topologies inferred by aforementioned MP, ML and IB analyses, we carried out the tip-dating analysis by neither fully relying on the stratocladistics approach nor completely fixing the tree topology. Instead, we adopted a compromise strategy to constrain the lineage topology which is simultaneously supported by MP3T, ML3 and BI3, and stratocladistically inferred the incongruent results across these undated analyses. The informative prior to the base of the clock rate is based on the non-clock BI3 analysis. Firstly, we calculated the median value for tree height in substitutions from posterior trees divided by the mean age value of the distribution of the root prior parameters: 8.947518/224.95 = 0.04; then, the mean for the lognormal distribution is: ln (0.04) = -3.2189 and the broad standard deviation for the lognormal distribution is: $e^{0.04}$ = 1.0408 (Simoes et al. 2020a, Simoes et al. 2020b). For rates sampled from a gamma distribution, the mean of the gamma distribution was also taken from the BI3 estimate (mean = 0.04), and a broad standard deviation = 0.5 was provided (Simoes et al. 2020a, Simoes et al. 2020b).

The sampling strategy for taxa was set to "diversity" (fossils assumed to be sampled randomly whereas extant taxa assumed to be sampled in a way to maximize diversity, and fossils can be tips or ancestors), which is standard practice in studies of higher-level taxa to diversified sampling of extant taxa (Zhang et al. 2016), and has been tested as a better fit to the data than others during the time estimate (Höhna et al. 2011). We fixed one rate-shifting time to 66 Ma, the K-Pg boundary with a mass extinction event. The sampling proportion of extant mantispoid taxa was set to 0.080, based on 42 terminals for ca. 528 extant species (Oswald 2022). The age of each fossil sample was assigned a uniform prior with lower and upper bounds from their corresponding stratigraphic range which was downloaded from the *Paleobiology Database* (https://paleobiodb.org/), to avoid biases in divergence time estimates introduced by single point age calibrations (Barido-Sottani et al. 2019, Simoes et al. 2020b). The root age was assigned an offset exponential prior (Zhang and Wang 2019, Simoes et al. 2020a). The minimum age of the offset exponential prior was set to the lower bound of the stratigraphic range of the oldest lance lacewing, †*Petrushevskia borisi* Martynova and †*Sogjuta speciosa* Martynova (Early Jurassic (Hettangian/Sinemurian)) = 201.3 Ma (Martynova 1958, Oswald 2022). The mean age of this prior was set to the previous median estimate for the divergent node of Osmyloidea and its sister lineage (node 179) = 248.6 Ma (Vasilikopoulos et al. 2020). The remaining priors and their parameters for SFBD were the default in MrBayes v. 3.2.7a or the referenced settings (Zhang and Wang 2019, Jouault et al. 2021) (Figs. 2, 3a; Supplementary Figs. S62, S64; see more detailed settings on Dryad at https://doi.org/10.5061/dryad.h18931zth).

Except for the estimations based on the unpartitioned setting, we also subdivided the dataset (232 characters) into four distinct functional partitions to explore their rate heterogeneities: head and prothorax (HP, 35 characters, raptorial system), foreleg (70 characters, raptorial system), pterothorax and wings (PW, 76 characters, flying system), and genitalia (51 characters) (Zhang and Wang 2019). Tree topology was constrained as in the unpartitioned analysis. The root age was fixed to be 256.4681 Ma (the median estimate of the root age in the unpartitioned time tree) in order to weaken the impact of systematic error (i.e., possible overestimate of ages of root and deep nodes in partitioned data) (Zhang and Wang 2019, Simoes et al. 2020a) on the following analyses (Fig. 3a; Supplementary Figs. S63, S65-S68; see more detailed settings on Dryad at https://doi.org/10.5061/dryad.h18931zth).

The convergence and mixing of the MCMC chains were evaluated in Tracer v1.7.2 and R package "convenience", to ensure the multiple runs converged on the same distribution and ascertain that effective sample sizes (ESS) exceeding 200.

We randomly selected 24 trees respectively from the unpartitioned and partitioned posterior time tree samples. We determined the mean rate of all branches at each 1 Ma interval respectively for overall Mantispoidea, Berothidae, raptorial Mantispoidea, Rhachiberothidae, †Dipteromantispidae and Mantispidae, from their origin age to 0 Ma or their exact extinction age. The mean rates from all 24 trees were then summarized at each time point using the median, upper (3/4), and lower (1/4) quartiles (Fig. 3b, c; Supplementary Fig. S69a-e) (Yu et al. 2023).

Phylomorphospace and Morphospace Analyses

The phylomorphospace comparisons were performed in R 4.1.2, based on the entire character matrix used for divergence time estimations, and other four anatomical cladistic matrices separated from it as in partitioned divergence time estimation. However, considering the substantial fraction of missing data generally above 25% on both empirical and simulated datasets reduces the overall distance between taxa that can be represented on ordination spaces (Lloyd 2016, Sutherland et al. 2019), we firstly calculated the proportions of true missing data ("?") in each cladistic matrix. Subsequently the genitalia character matrix was abandoned for analysis, which includes 51.14% true missing data (much larger than 25%). Furthermore, the cladistic matrix excluding genitalia characters was made to detect the impact of the missing data. We also removed the taxa with the proportion of missing data more than 50% in every cladistic matrix to further weaken the affect.

The function "ordinate_cladistic_matrix" in the R package Claddis v. 0.6.3 (Lloyd 2016) was utilized to construct the distance matrix and execute the principal coordinate analysis (PCoA) for each dataset. We conducted our analysis using the Maximum Observable Rescaled Distance (MORD) matrix, which can improve fidelity in datasets with high percentage of missing data (Lloyd 2016). The pre-OASE1 approach was employed to extend our sample size by including internal nodes through ancestral state reconstructions, which is the best phylomorphospace method to display realistic amounts of phylogenetic signal, rate heterogeneity, and convergent evolution (Lloyd 2018), and the partitioned clock-based tree (totally binary) with taxa pruned based on the corresponding dataset was inputted simultaneously. We regarded characters with inapplicable data (namely gaps ("-")) as secondary characters which relying on independent ones, creating an explicit linkage between them using the strategy in Hopkins and St John (2018). We created a two-column matrix for "dependent character" and "independent character" and set "inapplicable behaviour = "hsj", alpha = 0.5 (default)" in "ordinate cladistic matrix" function. The mean of each possible difference was taken both in the true polymorphisms (multiple states are observed in the taxon) and uncertainties, and Cailliez's correction was implemented for negative eigenvalues. Phylomorphospace grouping was mainly based on the current phylogenetic results and across time bins. Considering the potential erroneous phylogenetic signals and the morphospace compaction resulting from the phylomorphospace approach (Yu et al. 2021), we also performed a morphospace analysis without ancestral states reconstruction for comparison.

Measurements for Phylomorphospace and Morphospace

The size of morphological occupation/disparity, independence and relative position of different taxonomic groups can be observed directly in the phylomorphospace 3D graphics. The volume of convex hull (Fig. 4a, b; Supplementary Figs. S7a, d, g, S70-S72 and corresponding web links of 3D graphics, Table S4,) was calculated using the functions in the R package dispRity v. 1.6.8. However, since these graphics and volumes are based only on the first three PCoA score axes, which together explain less than 50% of the total variance, they provide limited and potentially biased information. Therefore, it is necessary to introduce the post-ordination metrics and statistical analyses to maximize the accuracy and reliability of our characterizations of variation in the dataset.

We used one post-ordination metric as a proxy for morphological disparity of different taxonomic groups or time bins — the sum of the variances (SOV, an important and powerful analytical tool to represent the occupation size, not sensitive to the sample size) (Wills et al. 1994, Korn et al. 2013, Hopkins and Gerber 2017). The PCoA scores of all axes were used to calculate this disparity metric. We simulated the random distribution of SOV under 100 bootstraps respectively for different taxonomic groups and time bins (Supplementary Figs. S71, S72, S75). We also employed the R package dispRity v. 1.6.8 to subdivide the phylomorphospace PCoA scores across time bins (25 Ma for Rhachiberothidae, 20 Ma for †Dipteromantispidae, 15 Ma for Mantispidae and 10 Ma for the remaining) and display the dynamics of morphological disparity (SOV) respectively for overall Mantispoidea, raptorial Mantispoidea, Berothidae, Rhachiberothidae, †Dipteromantispidae and Mantispidae (Fig. 4c-e; Supplementary Fig. S7b, c, e, f, h).

To determine whether different taxonomic groups or time bins of mantispoids occupy significantly different morphospace areas, we used a one-tailed permutational multivariate analysis of variance (PERMANOVA) (Anderson 2001, Yu et al. 2021) test on the original distance matrices with 10000 permutations under the “adonis2” function from the package vegan v. 2.5.7 (Dixon 2003) to calculate the null distribution of pseudo F ratio and p-value. All results are given in Supplementary Table S6. Permutation tests with sample size corrected (two tailed) were performed for each dataset across different taxonomic groups and time bins to assess whether there are significant differences in morphological disparity (SOV difference as the test statistic) among them, all against the null hypothesis of no difference (Yu et al. 2021) (see more details in Supplementary Appendix I).

We employed the geometric double-entity model (GDEM) to recognize far-near relations and independence (overlapping or not) of high-dimensional PCoA clusters. We measured this using the relative border distance (R_{AB}, a contrast between absolute border distance (D_{AB}) and dense degrees of samples in border regions, based on Euclidian distance) (Wang et al. 2011). We calculated R_{AB} using all axes of PCoA scores. This approach was necessary because in a high-dimensional dataset, the visualization methods based on dimension reductions usually cause some clusters to overlap, interlace, or be pushed away, resulting in incorrect or indistinguishable far-near relations. Moreover, the curse of dimensionality is present in any datasets with more than ten dimensions (Verleysen and Francois 2005, Clarke et al. 2008, Wang et al. 2011). Because each PCoA scores matrix in the present study has more than ten dimensions, we only used the nearest propagation method as the proxy for the degree of regional density. The detailed theory and derivation of GDEM can be seen in (Wang et al. 2011). All results are given in Supplementary Table S7.

All these analyses above were implemented in R 4.1.2.

Ancestral State Reconstruction

To further investigate the evolutionary patterns of the traits associated with raptorial lifestyles in deep time, we selected 34 representative discrete characters from the head, prothorax, foreleg and wings for ancestral state reconstruction. The new matrix was created based on the morphological dataset used in the phylogenetic analysis. This was done by directly selecting characters or combining inapplicable ones with those on which they depend. Maximum likelihood reconstruction of ancestral states was performed, based on the partitioned clock-based tree as input, using the function "ace" (the "two-pass" algorithm (much faster than stochastic mapping while having very close estimates)) in R package ape v. 5.6.2. Akaike's Information Criterion (AIC) was used to assess the best-fit model from "ER", "SYM" and "ARD" models for each selected character. The "ER" and "SYM" models performed better than "ARD" model for most characters. The "ER" model is given priority, when its AIC value is the same as for the "SYM" model, considering that both share similar result and the "ER" fits more characters best (See details in Supplementary Table S13). The results are shown on the phylogenetic tree edited in R 4.1.2 using phytools v. 0.7.90 (Supplementary Figs. S77-S110).

Furthermore, we reconstructed ancestral states of five continuous characters: (i-ii) the body size (using mean forewing length as the proxy (MF), also using amber maximum plus compressed fossil and extant minimum forewing length as the proxy (MmF) to weaken the bias caused by amber preservation that small individuals are more frequently preserved than large ones), and (iii-v) the comprehensive PcoA scores (CPS) from morphospace analysis (i.e., sum of the products of the PcoA scores and their corresponding variance contribution rates) as the proxy of overall morphological state of HP, foreleg and PW of each taxon. We used the contMap function in phytools v. 0.7.90 to perform this analysis. (Fig. 4h; Supplementary Figs. S111-S115).

Subsequently, we repeated the reconstruction of the five continuous characters above onto 24 randomly selected trees from the partitioned posterior dated tree samples. We determined the values of all ancestral nodes at each 1 Ma interval, respectively for overall Mantispoidea, Berothidae, raptorial Mantispoidea, Rhachiberothidae, †Dipteromantispidae and Mantispidae, from their origin age to 0 Ma or their exact extinction age. To enable reconstruction, it is necessary to ensure tree branch lengths greater than 0. Therefore, we replaced all branch lengths of 0 in each sampled tree with 1×10^{-6}, a value much smaller than the minimum evolutionary time unit—1 Ma. The mean value from all 24 trees were then summarized at each time point using the median, upper (3/4), and lower (1/4) quartiles (Fig. 4f, g; Supplementary Figs. S6b-d, S115b). Notably, ancestral reconstruction of CPS can indicate the degree of deviation of overall morphological state of the specific anatomical region from the initial ancestral state (i.e., the initial CPS value). The positive and negative signs of CPS values represent the different direction of the morphological evolution, while the difference from the initial CPS value indicates the degree of deviation. Greater deviation from the initial CPS value indicates a larger morphological difference from the ancestor, characterized by more apomorphic characters (novelties).

Diversification Rate Analyses

The partitioned time tree (completely binary) was input in BAMM v. 2.6 (Mitchell et al. 2018) to estimate diversification rates along tree branches and dynamics through time. The function

"setBAMMpriors" in the R package BAMMtools v. 2.1.8 (Rabosky et al., 2014) was used to generate the appropriate priors. We performed two independent Markov chains for 20 million generations. The breaks method option was set to "quantile method". The function "plotRateThroughTime" was used to plot the diversification rates over time respectively for Mantispoidea, raptorial Mantispoidea, Berothidae, Rhachiberothidae, †Dipteromantispidae and Mantispidae. The distinct shift configurations and their posterior probabilities were estimated, and the 95% probability shift scheme was summarized with the function "credibleShiftSet" (Fig. 5a-c; Supplementary Figs. S119; other settings seen in Supplementary Appendix 1 and Dryad at https://doi.org/10.5061/dryad.h18931zth).

To detect the intrinsic factors and putative environmental conditions responsible for the rise and demise of overall Mantispoidea, Berothidae, raptorial Mantispoidea, Rhachiberothidae, †Dipteromantispidae and Mantispidae, initially, we examined nine biotic and six abiotic variables, also called proxies (Lehtonen et al. 2017, Jouault et al. 2022a) (see details and reasons in Supplementary Appendix 1). Subsequently, a multivariate birth-death model (MBD) (Lehtonen et al. 2017) with both exponential (*-m 0* option) and linear (*-m 1* option) correlations was performed to test what extent biotic and abiotic factors can explain temporal variation in speciation and extinction rates in the program PyRate (Silvestro et al. 2015b). The lineage diversity through time plots were calculated in PyRate, using the age information of 24 trees from the partitioned posterior time tree samples (Fig. 5d). Subsequently, for the MBD analyses, we extracted the ages of nodes and tips as the times of speciation (Ts) and extinction (Te) from the partitioned time-calibrated phylogeny of Mantispoidea to create six "*Ts-Te*" files (see details on Dryad at https://doi.org/10.5061/dryad.h18931zth). Considering the potential biases in MBD estimation caused by non-corresponding nodes arising from differing tree topologies among the posterior tree samples, our analysis only extracted the lower, upper, median, and mean age values of all nodes and tips from the final partitioned time tree. We summarized the results of the MBD analyses by calculating the posterior mean, 95% HPD of all correlation parameters and the mean of the respective shrinkage weights ($\omega\lambda$, $\omega\mu$), as well as the mean and 95% HPD of the baseline speciation and extinction rates (Figs. 5e-i, 7a-d; Supplementary Figs. S119-S124; Supplementary Table S9). The MBD correlations are considered strongly significant only when fulfilling the double condition $\omega>0.5$ and $G\neq 0$, and when fulfilling only one of the criteria, and it suggests that there is either a weak support ($\omega< 0.5$) for a potential strong effect (95% HPD different from 0) or a strong support ($\omega> 0.5$) for a potential small effect (95% HPD crossing 0).

To further assess the effect of inter- and intra-lineage interactions on the diversification of four mantispoid families, we applied the multiple clade diversity dependence model (MCDD), a diversity-dependent model, with both exponential (*-m 0* option) and linear (*-m 1* option) correlations (Silvestro et al. 2015a). The "*Ts-Te*" files from the MBD analysis, were utilized as input files. We computed mean and 95% CI of the baseline speciation and extinction rates (λi and μi), the within-clade diversity-dependence parameters $g\lambda_{ii}$ and $g\mu_{ii}$, and the between-clade diversity-dependence parameters $g\lambda_{ij}$ and $g\mu_{ij}$. We used the mean of the sampled diversity-dependence parameters as a measure of intensity of competition or positive interaction between each pair of families (Fig. 7e; Supplementary Table S10). The interactions were considered significant when their median was different from 0 and the 95% CI did not overlap with 0.

The detailed information on settings for the MCMC iterations for the analyses above can be seen on Dryad at https://doi.org/10.5061/dryad.h18931zth. The first 10% of samples were discarded

as burn-in in each analysis. The convergence and mixing of the MCMC chains were all evaluated in Tracer v1.7.2 and R package "convenience", to ensure the multiple runs converged on the same distribution and ascertain that effective sample sizes (ESS) exceeded 200.

Post-hoc Assessment of Sampling Bias Effects

Considering the abrupt and anomalous changes observed in morphological disparity, body size, and diversification rates near the mid-Cretaceous, and given the extremely high sampling of Myanmar Kachin amber from the same period, we conducted a post-hoc assessment by excluding all samples from Myanmar amber for re-analysis to test, quantify and understand the potential biases. For morphological disparity, we selected only the dataset of overall morphological characters as an example for the test, given the high similarity of results across different anatomical regions (Supplementary Fig. S125). Regarding diversification rates estimated by fossil-BAMM, we focused on the time-rate curves of Mantispoidea in terms of the more distinct variations compared to those of other taxonomic groups (Supplementary Fig. S126). In the case of body size (Supplementary Fig. S115) and the diversification rates with the MBD model (exponential model as an example) (Supplementary Figs. S127-S129), we conducted repeated analyses after excluding all taxa from the Myanmar amber. Additionally, we did not include †Dipteromantispidae in these tests, as only two species remain after exclusion, which are insufficient to support the analysis.

RESULTS

Morphological Phylogeny

Primary results from present the phylogenetic analyses are outlined below (Fig. 2; Supplementary Figs. S3-S5, S60, S61; see details in the Supplementary Appendix 4). (i) Berothidae was recovered as a paraphyletic group (major clades: BM1, BM2), with Cyrenoberothinae and most of the Mesozoic genera resolving as the closest relative of raptorial Mantispoidea. †*Berothone*, †*Khasurtoberotha* and †*Mesithone* were transferred to Mantispidae. (ii) The monophyly of raptorial Mantispoidea, including Rhachiberothidae, †Dipteromantispidae, Mantispidae, and a stem group †*Archarhachiberotha*, was well-supported. (iii) The monophyly of Rhachiberothidae with Symphrasinae excluded was consistently recovered, while †Paraberothinae received limited support as a monophyletic group. (iv) †Dipteromantispidae was assigned as sister to Mantispidae. (v) The monophyly of Mantispidae was corroborated. The family comprises four monophyletic subfamilies, i.e., Symphrasinae, †Doratomantispinae, Calomantispinae, and Mantispinae (latter three subfamilies respectively form a monophylum, together with Drepanicinae, †*Haplacantha*, and †*Aragomantispa*, named as TPM). (vi) Drepanicinae and †Mesomantispinae respectively are paraphyletic. Many genera of †Mesomantispinae were recovered as basal lineages in the family. †*Acanthomantispa*, †*Dicranomantispa* and †*Psilomantispa* (originally placed in Drepanicinae), together with †*Pectispina* consist of a derived lineage in †Doratomantispinae. The extant drepanicine genera, Calomantispinae, and Mantispinae form a monophylum, named as DCM.

Divergence Time Estimation

Mantispoidea was estimated to have originated near the beginning of the Middle Triassic (ca. 246.6 Ma, HPD 377.4–219.1 Ma), with major lineages (all berothid lineages and raptorial families)

radiating from the Late Triassic to the Early Jurassic (231.3 (HPD 350.3–208.4 Ma) -183.0 (265.6–167.6 Ma) Ma). The raptorial mantispoids diverged from the closely related berothids near the T-J boundary (202.4 (HPD 314.1–183.9 Ma)-197.4 (HPD 300.3–180.5 Ma) Ma). The time-span from the Middle Jurassic to the mid-Cretaceous marked the peak for the origin and rapid radiation of mantispoid subfamilies and genera, particularly during the Early Cretaceous. Besides a great many Mesozoic lineages, the divergences of some Cenozoic lineages also traced back to the Cretaceous, while the remaining Cenozoic lineages originated from the Paleocene to Miocene (Fig. 2; Supplementary Figs. S62, S63, Tables S2, S3).

Morphological Evolutionary Rates

In the unpartitioned tree of Mantispoidea (Fig. 3a; Supplementary Fig. S64), early divergences show moderately to extremely high evolutionary rates (2.00-17.38). The highest rate (17.38) is found during the early radiation of raptorial Mantispoidea. High rates (>2.00) were also frequently observed after the early rapid evolution, particularly in Mantispidae clades exhibiting more moderately to extremely high rates (2.00-14.63). The overall evolutionary rate curves for each taxonomic group either had peaked or reached their peak within a short period (<10 Ma) during their early evolution, then followed by the overall declining trend with numerous fluctuations (Fig. 3b).

In the partitioned trees (Supplementary Figs. S65-S68), high rates for the head-prothorax partition (HP) are observed during the early diversification of raptorial Mantispoidea and within Mantispidae. The pterothorax-wings partition (PW) shows high rates in the early-diverging mantispoid lineages, †Dipteromantispidae, and Mantispidae. The foreleg partition exhibits high rates within raptorial Mantispoidea, which is also the sole partition with extremely high rates (34.11, 25.03). The evolutionary rate curves of some anatomical regions reached the peak much later than the clade origin time, such as HP in Rhachiberothidae and PW in Mantispidae, Rhachiberotidae, and Berothidae. A second or more distinct peak in the evolutionary rate curve occurs in the HP rates of Mantispidae and Rhachiberothidae, and the foreleg rates of Mantispidae. The evolutionary rates of raptorial groups throughout the Mesozoic, except †Dipteromantispidae and PW of Rhachiberothidae, are generally at a higher level than Berothidae.

Morphospace and Disparity

We compared the morphospaces of different anatomical regions among mantispoid lineages to quantitatively infer the patterns and extent of morphological variation throughout their evolutionary history (Fig. 4a, b; Supplementary Figs. S7a, d, g, S70-S74; Tables S6, S7). Raptorial Mantispoidea occupy a larger morphospace in overall morphology and anatomical regions than Berothidae. Mantispidae has the largest morphospace among mantispoid families, while †Dipteromantispidae has the smallest (except its foreleg and PW morphospace). Rhachiberothidae only displays a larger foreleg morphospace than Berothidae. Morphospace differences are generally significant among mantispoid higher-level taxa, but with slight overlap in the HP or PW morphospace for some groups. Generally, the morphospace of later diverging lineages show greater distances than the earlier diverging lineages and vice versa, except for some groups with highly specialized characters, such as †Dipteromantispidae (specialized PW) and Symphrasinae (specialized foreleg).

A rapid expansion of disparity took place during the early evolution of each mantispoid groups, and it remained stable until the Late Cretaceous (around 100 Ma), followed by a distinct drop or extinction (Fig. 4c, e; Supplementary Fig. S7b, c, e, f, h, S75, S76; Table S5). This decline in raptorial mantispoids was notable, leading to significantly smaller disparity in Paleogene and Neogene than in the Cretaceous. After this decline, the disparity of most groups increased again, except for †Dipteromantispidae, which went extinct. The disparity of extant Rhachiberothidae is generally lower than that in the Cretaceous. After excluding the high density of samples from the Myanmar amber, the dramatic decline around 100 Ma in morphological disparity was attenuated and noticeably delayed in entire Mantispoidea, Berothidae and raptorial Mantispoidea, and completely disappeared in Mantispidae (Fig. 4d; Supplementary Fig. S125a-c, e). In Rhachiberothidae, the inflection point occurred earlier, around 125 Ma (Fig. 4d; Supplementary Fig. S125d).

Evolution of Raptorial Foreleg Traits and Body Size

We demonstrated that the raptorial lifestyle in Mantispoidea has a single origin (Supplementary Figs. S6a, S86-S109). The foreleg of raptorial Mantispoidea initially underwent high morphological complexification, which was enhanced further within Rhachiberothidae and Mantispidae via convergent evolution. This is featured by the wider and thicker profemur, the larger and stiffer profemoral ventral ISs, and the diverse specialized setae of the protibiae and protarsi (Supplementary Figs. S6a, c, S86-109, S112. However, this structure (particularly in the derived lineages) also shows a trend of reduction during the subsequent evolution. This is marked by the simplification of profemoral ISs with larger ones outstanding, the reduction or loss of specialized protibial and protarsal setae, and the reduction of pretarsal claws and arolium (see more results in Supplementary Appendix 5).

In the early evolutionary stages of raptorial Mantispoidea, the overall morphology of the forelegs exhibited a much more significant deviation from the initial ancestral state of Mantispoidea (with a much greater number of novelties) than that of Berothidae (Supplementary Fig. S6c). Both Rhachiberothidae and Mantispidae exhibited positively deviating foreleg morphology, peaking around the mid-Cretaceous. However, in Rhachiberothidae, it quickly dropped back to the initial state, while in Mantispidae, the decline began near the K-Pg boundary. In contrast, the morphological novelties in the raptorial forelegs of †Dipteromantispidae remain minimal, without significant fluctuations.

The body size of Berothidae and Rhachiberothidae decreased after their origin, and began to increase stably respectively from the Early Cretaceous and the late Jurassic to the present (Fig. 4f), slightly exceeding the ancestral body size during the mid-Cretaceous. In contrast, Mantispidae maintained a larger body size than all other mantispoid families throughout their evolutionary history. Similar to Berothidae, the body size of Mantispidae reached the lower point in the Early Cretaceous and then steadily growing to the present (Fig. 4f; Supplementary Fig. S6d).a notably increasing body size was found in the BM1 clade and Mantispidae, while BM2, Rhachiberothidae, and †Dipteromantispidae were observed to have undergone distinct miniaturization (Fig. 4h). The dramatic elevation of body size during 125 – 100 Ma attenuated substantially in Mantispoidea, Berothidae, raptorial Mantispoidea and Mantispidae, after excluding all samples from the Myanmar amber (Fig. 4g; Supplementary Fig. S115b).

Dynamics of Diversification

Fossil-BAMM results suggest that the significant rate shifts are observed in the divergence between raptorial Mantispoidea and Berothidae, †Dipteromantispidae and the DCM clade (Fig. 5a-c, Supplementary Figs. S116-S118). The diversification of most Mesozoic raptorial lineages was characterized by high speciation rates alongside high extinction rates, which results in generally low net diversification rates. In contrast, most Cenozoic raptorial lineages diversified at higher net rates, particularly within Mantispinae. When all Myanmar amber samples were removed, the pattern of diversification rates mapped on the phylogenetic tree showed almost no change (Supplementary Fig. S126a, c, e).

Lineage diversity began to decline across all families during the Early Cretaceous, with †Dipteromantispidae extinct by the Late Cretaceous (Fig. 5d). While the diversities of Berothidae and Mantispidae in the Neogene surpassed their Cretaceous levels, Rhachiberothidae, despite some recovery, remained stagnant. The temporal rate dynamics estimated by fossil-BAMM in raptorial groups is limited and show minimal fluctuation (Supplementary Fig. S119), possibly due to its focus only on the major, infrequent events that affected diversification and the effects of small extinct phylogenetic dataset (Alfaro et al. 2009, Maliet et al. 2019, Černý et al. 2021). In contrast, the MBD model performs much better (Fig. 5e-i; Supplementary Fig. S120a-c, S121-S123). The results under the exponential model and the linear model are similar, but the latter displays more gradual curves than the former, except for the result of †Dipteromantispidae. All taxonomic group originated with very high speciation and net diversification rates. In Berothidae, raptorial Mantispoidea, Rhachiberothidae and Mantispidae, early speciation rates and net diversification rates were the highest throughout their entire evolutionary histories. Although there were many fluctuations and elevations in subsequent evolution, they never returned to their early evolutionary peak. In †Dipteromantispidae, though these two rates were also relatively high in the early stages of evolution, their peak occurred around 150 Ma. A significant shift in net diversification rates across all groups is observed in the mid-Cretaceous, and a similar shift in speciation rates is observed across all groups except for the entire raptorial Mantispoidea. In Berothidae, raptorial Mantispoidea, Rhachiberothidae, and †Dipteromantispidae, the early extinction rates generally remained at a relatively low level, with distinct shift and peak values often occurring during the mid-Cretaceous. However, the extinction rate was highest at the origin of Mantispidae and subsequently showed an overall declining trend, with no significant changes during the mid-Cretaceous. Our study also suggests a pattern of widespread synchronous rises and declines between speciation and extinction rates. Notably, when excluding numerous samples from the Myanmar amber, the striking shift around the mid-Cretaceous disappeared or significantly weakened (Fig.6; Supplementary Figs. S127-S129).

The results of correlation tests under exponential and linear models are almost consistent, but the former model detected more factors with potential strong effect or high support (Fig. 7a-d; Supplementary Fig. S124). Here we summarized the results under the exponential model. We identified nine variables with potential strong effect or high support on Mantispoidea (Fig. 7a): (i) negative effect of intrinsic diversity on extinction, (ii) positive effect of foreleg novelties (CPS) on extinction, (iii) negative effect of foreleg rates on speciation and extinction, negative effect of (iv) PW novelties and (v) PW rates on extinction, (vi) negative effect of Angiosperm on extinction, (vii) negative effect of magmatism on speciation, (viii) negative effect of sea level on extinction and (ix) positive effect of temperature on extinction. Two variables with potentially strong effect

were identified on Berothidae (Fig. 7b): (i) negative effect of intrinsic diversity on speciation, and (ii) negative effect of magmatism on speciation and extinction. Four variables were identified with potentially strong effects on raptorial Mantispoidea (Fig. 7c): (i) negative effect of PW novelties on extinction, (ii) positive effect of temperature on extinction, negative effect of (iii) PW rate and (iv) sea level on extinction. The rate of PW was identified as a negative effect on extinction on †Dipteromantispidae, with both potentially strong effect and high support (Fig. 7d). Notably, we did not directly conclude that PW morphology correlates positively with extinction rate. Instead, we consider it to correlate negatively, because the proxy (CPS values) of PW generally increases (greater deviation) in a negative direction across time.

The results of the MCDD analyses under exponential and linear models are almost consistent, but the former model identified more significant interaction events with higher mean value of the parameters (Fig. 7e; Supplementary Table S10). Here we summarized the results under the exponential model. Both negative and positive intra-clade interactions in Berothidae, †Dipteromantispidae and Mantispidae were supported by the MCDD analysis. Only in Mantispidae, the positive effect of speciation rates is much greater than the negative effect of extinction on the intra-clade interactions. MCDD analysis further shows increasing Berothidae diversity correlated with lower extinction in †Dipteromantispidae and Mantispidae, and with higher speciation in Mantispidae; increasing Rhachiberothidae diversity correlated with higher speciation in Berothidae, and with higher extinction in Mantispidae; increasing †Dipteromantispidae diversity correlated with higher extinction in Berothidae and Mantispidae, and with higher speciation in Mantispidae; increasing Mantispidae diversity correlated with both higher speciation and extinction in Berothidae, lower speciation in Rhachiberothidae, and higher extinction in †Dipteromantispidae.

DISCUSSION

Our study delves into the role of evolutionary novelties in diverse predatory specializations of Mantispoidea across deep time, along with the comparisons of strikingly divergent evolutionary trajectories among different families as a natural experiment. We demonstrate that evolutionary novelties can act as a double-edged sword, exerting a more complex impact on lineage diversification than previously understood. The development of novelties that focused on a specific anatomical area can initially confer significant advantages but time and environment may dull their edge, sometimes causing groups to become canalized into a narrow ecological corner, or even terminate. Conversely, ecological breadth and/or diverse novelties may circumvent the fate that befalls overspecialized relatives. Moreover, morphological evolution may have the same or different effects respectively on speciation and extinction rates, thereby intricately influencing lineage diversification. These aspects of evolutionary novelties are often overlooked when traits are linked to putative adaptive radiations. The interplay between evolutionary novelties and lineage diversification in Mantispoidea through time and among lineages is further elaborated below.

Early Adaptive Radiation of Raptorial Mantispoidea

The emergence of the raptorial foreleg is believed to be the primary catalyst for an early adaptive radiation of raptorial Mantispoidea from the Late Triassic and the Early Jurassic, with a series of key innovations linked to predatory behaviour (i.e., more elongate procoxa, incrassate

profemur, fully developed profemoral ventral ISs, and curved protibial base) (Fig. 2). The results of our analyses demonstrate during this period: (i) much higher overall evolutionary rate in raptorial Mantispoidea than in Berothidae, with much higher foreleg rate than other anatomical regions (Fig. 3a-c; Supplementary Figs. S64-69); (ii) dramatically increasing morphospace in raptorial Mantispoidea, which rapidly surpassed that of Berothidae, with greater surpassing degree in foreleg morphospace (Fig. 4c-e; Supplementary Fig. S7b, c, e, f, h); (iii) foreleg serving as the main contributor to the morphospace isolation of raptorial Mantispoidea from Berothidae (Fig. 4a, b; Supplementary Fig. S7a, d, g; Supplementary Table S7); (iv) the enlargement of body size in raptorial Mantispoidea (Fig. 4e, f), and (v) speciation (both fossil-BAMM and MBD) and net diversification rates (MBD) of the raptorial Mantispoidea beginning at a significant high level, which had usually surpassed the contemporaneous Berothidae before the mid-Cretaceous (Fig. 5a, e, f). Although the fossil-BAMM result shows different results in net diversification rates (Fig. 5c; Supplementary Fig. S119b, c) from MBD, this does not overshadow the consistent support from other macroevolutionary parameters for the significant impact of the raptorial foreleg during the early evolution of raptorial Mantispoidea.

After the origin of cursorial mantispoids (berothids), a decline in evolutionary rates, speciation and net diversification rates, increase in extinction rate, and slow variation in disparity and body size were observed (Figs. 5b, c, f-i, 4e; Supplementary Figs. S7b, c, e, f, h, S69, S119b). These trends and the negative effect of intrinsic diversity on speciation (Fig. 7a, b, e) suggest a potential ecological niche overlap and saturation of niche space, likely leading to intense competition within berothids (Stroud and Losos 2016, Benson 2018, Pastore et al. 2021). Therefore, under this evolutionary stalemate, the advent of predatory specializations associated with the raptorial foreleg allowed the originally omnivorous or palynophagous mantispoid adults (Devetak and Klokocovnik 2016) to exploit broad carnivorous ecological niches and break through the bottleneck of diversification of Mantispoidea.

The Impact of Evolutionary Novelties on Different Mantispoid Lineages Across Time

After the origin of the main lineages (Rhachiberothidae, †Dipteromantispidae and Mantispidae) of raptorial Mantispoidea, the aforementioned positive evolutionary impact of raptorial foreleg novelties was notably diminished, with greatly varied manifestations in the evolution of different lineages. In Rhachiberothidae, raptorial forelegs continued to be the primary factor driving their morphological evolution during the Mesozoic (Fig. 2), which is supported by the significantly high evolutionary rates only in the foreleg, a substantial contribution of the foreleg morphospace to the overall morphospace, a higher morphological deviation of the foreleg from the initial ancestral state of Mantispoidea (Figs. 3a-c, 4a-d; Supplementary Figs. S6b, c, S7, S69, S111-S113). Nevertheless, this preference for innovating raptorial foreleg did not promote the prosperity of Rhachiberothidae. This evolutionary bias might have limited the evolution of other anatomical regions and resulted in lineage constraint. This is evidenced by a generally high correlation among different anatomical regions in rates, disparity and novelties (CPS) (Supplementary Table S11), low overall evolutionary rates (Fig. 3a, b; Supplementary Fig. S64), declining speciation and net diversification rates before the mid-Cretaceous (Fig. 5g), as well as eroded, irrecoverable diversity and morphological disparity after the mid-Cretaceous (Figs. 4c-e, 5d, g). Additionally, the long-term maintenance of a small body size (Fig. 4f, g) may also reflect evolutionary pressure within Rhachiberothidae. Notably, the shift of evolutionary focus towards

HP and PW from the Late Cretaceous to the Cenozoic may have been a significant factor affecting the slight recovery of Rhachiberothidae.

In †Dipteromantispidae, the evolutionary emphasis shifted from the novelties of the raptorial foreleg to the pterothorax and wings (PW)—dipterization (Fig. 2), evidenced by the extremely high evolutionary rates only on PW (Fig. 3a; Supplementary Figs. S64-S69), the significant contribution of PW to the overall morphospace (Supplementary Figs. S7, S70), the main role of the PW in driving morphospace isolation (Supplementary Table S7), and the well-supported strong potentially negative effect of PW rate on extinction (Fig. 7d). This innovation sharing similar flight morphology with Diptera might have greatly enhanced the flight efficiency and agility of this group, thereby improving their foraging and migration as well as their ability to evade predators (Chan 1998, Dudley 2000, Faruque and Humbert 2010, Krishna et al. 2020), and thus this family extended into a completely new ecomorphospace distinct from other mantispoids (Fig. 4a). Such a bold evolutionary attempt might have significantly boosted the diversification of †Dipteromantispidae during their early evolution as a key innovation. This is evidenced by very high overall evolutionary rates, increasing high speciation and net diversification rates, long-term low extinction rates, and the larger body size than Rhachiberothidae before the Early Cretaceous (Figs. 3a, b, 4e, f, 5h). However, the evolutionary bias on the highly specialized PW might have further caused †Dipteromantispidae to face a scenario similar to that of Rhachiberothidae after ca. 150 Ma, ultimately contributing to its inability to survive the later mass environmental shift such as the Cretaceous Terrestrial Revolution (Lloyd et al. 2008, Benton et al. 2022, Peris and Condamine 2024), the Cenomanian-Turonian extinction event (Pearce et al. 2009, Forkner et al. 2021), etc.

Summing up the above, the evolutionary bias towards novelties of a specific anatomical region in a lineage may enhance and optimize certain traits and functions, as well as consolidate the ecomorphospace, under the stable environment. However, such evolutionary bias, whether it is towards the raptorial foreleg or not, may negatively influence long-term evolution. The flaw of evolutionary bias on one hand refers to the intensification of competition in a lineage with high similarity of innovative structures and ecological niche overlap (Abrams 1983, Burns and Strauss 2011, Roy et al. 2021). Although existing studies have shown that competition between species can promote evolutionary diversification through ecological character displacement and niche differentiation (Day and Young 2004, Grant and Grant 2006, Drury et al. 2018), evolutionary bias may impede this beneficial process by morphological constraint across time, thereby potentially exacerbating the negative impacts of competition. On the other hand, evolutionary bias may constrain the plasticity and flexibility, leading to the occurrence of more highly specialized and exaggerated structures, which may be energy-intensive and increase extinction risk when major environmental shifts take place (Futuyma and Moreno 1988, McKinney 1997, Emlen 2001, McGill et al. 2006, Clavel et al. 2011, McGee et al. 2015).

Conversely, Mantispidae seemingly achieved a balanced evolutionary pattern among morphological regions, with reduced bias for raptorial foreleg and increased modularity and plasticity in other regions, indicated by higher evolutionary rate, morphospace and state deviations for other regions, less evolutionary rate correlation among different regions, and weak correlation between morphology of foreleg and PW (Figs. 2, 3a-c, 4a-e; Supplementary Figs. S6b, c, S7, S69, S111-113; Supplementary Table S11). This strategy increases the opportunities for forming distinctly diverse innovations (Levis et al. 2018), enhancing the adaptability to environmental

changes, enabling expansion into brand new ecomorphospace to minimize the overlap within the lineage, and flexibly responding to the pressures from intra- and interspecific competition (Fig. 7e). These benefits are supported in mantidfly diversification dynamics by the higher overall evolutionary rates, the more rapid growth and highest overall morphological disparity among families, the largest body size throughout their evolutionary history, the highest speciation and net diversification rates during the early evolution, and no elevation of extinction rate in the Late Cretaceous (Figs. 3, 4, 5i). Additionally, Mantispidae are the sole raptorial family whose overall morphological disparity and lineage diversity in the Neogene recovered to a significantly higher level than in the Cretaceous (Figs. 4c, 5d).

Notably, such complex and diverse evolutionary innovations may be sufficient, but not essential for the evolutionary stability and success. In contrast to raptorial families, the innovations of Berothidae in subsequent evolution seem unremarkable and significantly fewer, maintaining long-term lower evolutionary rates both in overall morphology and in different anatomical regions. Although the evolutionary focus of Berothidae is on the innovation of HP and PW (Fig. 2), different anatomical regions still exhibit more modularity and plasticity than Rhachiberothidae and Dipteromantispidae, with some of them showing no correlation in either evolutionary rates or morphological disparity (Table S11). This evolutionary strategy, though not leading to remarkable diversification as seen in raptorial families over their histories, has made Berothidae maintain more stable diversification (long-term speciation and extinction rates lower than 0.05) and achieve greater overall morphological disparity than the strongly evolutionarily biased Rhachiberothidae and †Dipteromantispidae (Figs. 4c, 5d, e). This strategy might have allowed Berothidae to survive from the heavy competitive and predatory pressures of its raptorial relatives and multiple environmental changes, thereby persisting to the present at relatively high diversity.

The Complex Impact of Morphological Evolution on Diversification

The MBD analysis further suggests that the morphological evolution does not show a simple, positive or negative impact on lineage diversification (Fig. 7a-d). First, the morphological novelties or rates could have consistent impact on both speciation and extinction rates. For example, the increasing foreleg rates in entire Mantispoidea might have synchronously led to lower speciation and extinction rates (Fig. 7a). Second, the morphological novelties and rates together could have similar influence respectively on speciation or extinction rate. For instance, both of the PW morphological novelties and morphological rates might have negative impact on extinction rates in the entire Mantispoidea and raptorial Mantispoidea (Fig. 7a, c). However, the impacts of different morphological novelties or rates could also vary significantly on the same diversification rate. As shown herein, the foreleg novelties across Mantispoidea might have increased extinction rates, while higher morphological rates of foreleg might lead to lower extinction rates (Fig. 7a).

The above complex impacts of morphological novelties and rates on lineage diversification imply a dynamic balance of morphological evolution. Remarkably, not all novelties are beneficial for evolution. Some traits could be energy-consuming or unfavorable for survival (Futuyma and Moreno 1988, McKinney 1997, Emlen 2001, Clavel et al. 2011, McGee et al. 2015), and moreover, the excessive accumulation of similar characters could lead to niche overlap and intense competition (Abrams 1983, Burns and Strauss 2011, Roy et al. 2021), both of which may decrease

speciation rate or elevate extinction rate. Additionally, high evolutionary rates indicate more frequent alterations of morphological character states, leading to quicker accumulation of morphological diversity with more novelties, being either positive or negative. Sufficiently high evolutionary rates may allow for the prompt updating of novelties, and new adaptive traits can rapidly emerge to fill the ecomorphospace niche, thereby contributing to an increase in diversity (Simpson 1953, Kingsolver and Pfennig 2007, Rabosky 2014). Conversely, the slower evolutionary rates might result in specialized or similar traits not being promptly updated, reducing the likelihood of adaptive traits emerging, potentially leading to the ecological vulnerability and a decline in diversity. (Simpson 1953, Lynch and Conery 2000, Emlen 2001, Kingsolver and Pfennig 2007).

The Impact of Environmental Factors

Our MBD analysis demonstrates the non-negligible role of environmental factors, synergizing with evolutionary innovations, on the diversification of Mantispoidea. They may concurrently exert similar impacts on multiple different lineages, especially those with analogous evolutionary strategies. Previous studies (Nicholson et al. 2014, Smith and Marcot 2015, Condamine et al. 2016, Condamine et al. 2020, Jouault et al. 2022a, Jouault et al. 2022b, Peris and Condamine 2024) have highlighted the profound impact of the Permian-Triassic extinction event (PTE) (ca. 252 Ma) (Erwin 1994, Wignall 2001) on insect diversification. Considering the estimated root age of Mantispoidea at approximately 246.6 Ma, which is slightly postdating the mass extinction event, the potential impact of PTE should be noted. The MBD analysis indicate that there was a remarkable shift in the speciation, extinction and net diversification rates of the entire Mantispoidea and Berothidae around 252 Ma (Fig. 5e; Supplementary Figs. S120a-c, S121a, b, S122a, b, S123a, b). Moreover, the negative effects of this mass extinction event appear to have been short-lived, with the net diversification rate recovering rapidly in a brief period (<10 Ma) (Fig. 5e; Supplementary Figs. S120c, S123a, b), followed by high overall evolutionary rates (Fig. 3b; Supplementary Fig. S69a) and rapidly increasing morphological disparity. Thus, the rapid early radiation of Mantispoidea could be partially accelerated by the increase of substantial ecological niche due to the severe impact of PTE on the insect diversity that had accumulated previously, particularly during the Carboniferous period (Nicholson et al. 2014, Condamine et al. 2016, Condamine et al. 2020).

Our study did not detect a direct association between the well-known Carnian Pluvial Episode (234-232 Ma) (CPE) (Corso et al. 2020) in the Late Triassic and the diversification of the taxonomic groups within Mantispoidea. The significant shifts in speciation, extinction and net diversification rates all occurred before this event (Fig. 5e; Supplementary Figs. S120a-c, S121a, b, S122a, b, S123a, b), a result consistent with the existing studies on deep-time diversification of insects (Condamine et al. 2016, Condamine et al. 2020, Jouault et al. 2022b). However, the post-CPE impacts are still noteworthy, given that MBD analysis suggests a dramatic increase in net diversification rates following this event (Supplementary Figs. S120c, S123a, b), which may have also laid the foundation for the early adaptive radiation of raptorial lineages. The CPE event substantially increased global precipitation and humidity, alleviating Triassic aridity and boosting vegetation abundance with the rise of Bennettitales and modern conifers (Corso et al. 2020, Lu et al. 2021). This significant environmental changes may have provided opportunities for the

emergence and diversification of raptorial Mantispoidea, such as new ecological niches, available resources, and more suitable habitats.

Previous studies have indicated that the end-Triassic mass extinction event (ca. 200 Ma) (ETE) (Hautmann 2012) had no significant impact on insect diversity (Nicholson et al. 2014, Smith and Marcot 2015, Condamine et al. 2016, Condamine et al. 2020, Jouault et al. 2022a, Peris and Condamine 2024). Similarly, our study also indicates that this event may have had a less impact on mantispoid diversification. Even when an abrupt shift in speciation, extinction, or net diversification rates can be observed around this event, these changes are less pronounced than the shifts that occurred just before or shortly after the event. (Fig. 5e-i; Supplementary Figs. S120a-c, S121-S123). Additionally, we also do not detect a significant shift in the evolutionary rate, morphological disparity and body size around this event. Mantispoids may demonstrate remarkable resilience to the extinction and might have effectively grasped new ecological opportunities for recovery or adaptive radiation within a brief period.

The most significant evolutionary change across various mantispoid groups during the mid- to Late Cretaceous was characterized by remarkable declines and subsequent increase in lineage diversity and morphological disparity, notably high extinction rates, significant shifts of net diversification rates, and distinctly increasing body size (Figs. 4c-g, 5; Supplementary Figs. S7b, c, e, f, h, S120, S122, S123). Cenomanian-Turonian extinction event (ca. 93.9 Ma) in the Late Cretaceous (Pearce et al. 2009, Meyers et al. 2012, Forkner et al. 2021) may not contribute to all these dramatic changes, as they were estimated to occurr before this event. In contrast, the significant terrestrial vegetation turnover triggered by the explosion of angiosperms—marked by events such as the Angiosperm Radiation (125–90 Ma), the Cretaceous Terrestrial Revolution (125–80 Ma), and the Angiosperm Terrestrial Revolution (ATR, 100–50 Ma) (Lloyd et al. 2008, Benton et al. 2022, Peris and Condamine 2024)—may have been mainly responsible for the series of the notable changes in macroevolutionary parameters during the mid-Cretaceous. Apart from the initial extinction, the subsequent rapid rebound in net diversification rates, increasing morphological disparity, and larger body size reflect the resilience and recovery of mantispoid lineage diversification (Figs. 3b, c, 4c-g, 5d-i; Supplementary Fig. S7b, c, e, f, h, S69, S120c, S123). This may be explained by the augment of resources from the updated terrestrial vegetation for the mantispoid survivors after extinction, as well as the elevation of sea level leading to more geographical isolation during the Late Cretaceous (Fig.7a, c) (Snedden and Liu 2010, Peris and Condamine 2024). Nonetheless, due to particularly abundant fossil records from the mid-Cretaceous Myanmar amber and lower records from the Late Cretaceous and Cenozoic, sampling bias may also mislead the estimation of evolutionary dynamics and should be further evaluated when more fossil data beyond the mid-Cretaceous are available (Figs. 4d, g, 6; Supplementary Figs. S125-S129).

For the K-Pg extinction event (ca. 66 Ma) (Klein et al. 2021), the previous studies suggested that this event may have affected certain specific insect groups, but its long-term impact on overall insect diversity appears to be limited (Nicholson et al. 2014, Smith and Marcot 2015, Condamine et al. 2016, Condamine et al. 2020, Jouault et al. 2022a). Many insects demonstrated strong adaptability and still even maintained a high net diversification rate after this event (Nicholson et al. 2014, Smith and Marcot 2015, Condamine et al. 2016, Jouault et al. 2022a). Peris and Condamine (2024) mentioned that during the post K-Pg, diversification of insect and angiosperm mutually spurred each other, resulting in ecological dominance of angiosperms and the emergence

of new pollinating insect lineages. Likewise, this event appears to have had a less significant impact, and mantispoids may have also demonstrated great resilience and rapid recovery, because various evolutionary parameters, including morphological diversity, body size, lineage diversity, speciation, extinction and net diversification rates, showed little fluctuation around this event (Fig. 3b, c, 4c-e, 5d-i; Supplementary Fig. S7b, c, e, f, h, S69, S120-S123).

Complex Intra- and Inter-clade Interaction Networks

The complex intra- and inter-clade interaction networks inferred by MCDD analysis within Mantispoidea suggest that the increase in intrinsic diversity of the clade had bidirectional effects on species diversification, simultaneously inhibiting speciation rates while reducing extinction rates (Fig. 7e; Supplementary Table S10). This indicates a complex dynamic balance and regulatory mechanism in terms of intra-clade diversity. On the one hand, increasing species numbers, with enhancements in genetic and morphological diversity, might result in rapid niche filling and functional redundancy (Tilman 1999, Petchey and Gaston 2002, Gonzalez and Loreau 2009, Le Bagousse-Pinguet et al. 2019). These can enhance ecosystem stability and adaptability, provide a broad range of variations for natural selection, and reduce the extinction risk for the entire clade from a single disaster. On the other hand, similarity and overlap in ecological niches also enable intensive intra-clade competition, which may negatively impact the speciation rate (Abrams 1983, Schluter 2000, Gonzalez and Loreau 2009, Burns and Strauss 2011).

Similarly, such complex dynamics of mutual benefits and conflicts may be common in inter-clade interactions (Fig. 7e; Supplementary Table S10). Besides the increased extinction rates and decreased speciation rates which are caused by niche overlap and saturation led to intensive competition, the presence of raptorial forelegs across many taxonomic groups suggests that predator-prey relationships should also not be overlooked as well. Predatory behaviors may negatively affect the diversification of preys by direct reduction in their population sizes, alteration of their behavior and habitat use, and resulting in niche compression (Abrams 2000, Pangle et al. 2007, Creel and Christianson 2008, Griffin et al. 2013). However, they may also regulate the population expansion of preys, especially the dominants, filtering out disadvantageous variations or redundant groups with similar characters, ensuring accessibility to available ecological niches and modulating the trophic structure to promote the diversification of preys (Paine 1966, Abrams 2000, Chase and Leibold 2003, Terborgh 2015). Furthermore, the diversification of preys can enhance predator diversity primarily by ensuring a broader range of food sources, promoting the differentiation of predatory niches, triggering more varied selective pressures for the predators and simulating a predator-prey arms race (McCann 2000, Bascompte 2009, Holt 2009).

The degree of morphological bias may also impact on the inter-clade interactions. Specifically, we found that Rhachiberohthidae, which exhibits a strong preference for raptorial forelegs, has been found to only experience significant negative impacts from the diversification of Mantispidae, without any positive effects from the diversification of other clades. †Dipteromantispidae fared slightly better, benefiting only from the diversification of Berothidae, but this positive effect is much smaller than the adverse impacts from Mantispidae. In contrast, Berothidae and Mantispidae, which show more morphological balance and greater plasticity, not only suffered substantial negative effects from diversification of other clades but also gained more benefits.

Conclusions

Our exploration on the role of evolutionary novelty in lineage diversification using mantispoid macroevolution as a model has provided substantial insights. The novelties of the raptorial foreleg did trigger an early adaptive radiation from the Late Triassic to the Early Jurassic, where they acted as key innovations. However, the diverging evolutionary trajectories among major lineages of Mantispoidea over deep timescales was not solely dominated by novelties of this sophisticated structure. Over time, the positive influence of the raptorial foreleg on lineage diversification waned or even reversed. The flourishing of a lineage can be attributed to the innovation and plasticity of various anatomical regions, but the evolutionary bias towards a specific structure may lead to an evolutionary bottleneck.

Notably, the impact of morphological evolution on lineage diversification should not be simplistically categorized as either promotive or inhibitive. The complex effects respectively on speciation and extinction rates require detailed analysis to more deeply and comprehensively understand the mechanisms driving diversification. The broader Mesozoic environmental shifts and complex intra- and inter-clade interaction further compounded these dynamics, emphasizing the importance of external factors in shaping evolutionary trajectories. Additionally, to obtain more objective and reliable results, researchers are advised not to overlook the impact of sampling bias in macroevolutionary analyses, and to conduct pre- or post-hoc tests if necessary. This holistic examination underscores the multifaceted nature of evolutionary processes and the interplay between novelties and ecological factors in diversification.

SUPPLEMENTARY MATERIAL

Data available from the Dryad Digital Repository:
https://doi.org/10.5061/dryad.h18931zth

AUTHOR ACKNOWLEDGEMENTS

We appreciate Dr. Yongjie Wang, Dr. Dong Ren, Mrs. Xiumei Lu, Mrs. Jinglei Wang, and Mrs. Xiao Jia for sharing the information on mantispoid fossils. We thank Dr. Chi Zhang, Dr. Daniele Silvestro, Dr. Liang Lv, and Mr. Xianye Zhao for their valuable suggestions for optimization of our analytical methods. We are also grateful to Dr. Corentin Jouault and anonymous reviewers for their constructive comments.

AUTHOR CONTRIBUTIONS

X.Y.L. and H.Y.L. conceived the study. H.Y.L., D.Z., B.W., H.N., S.Y., W.W.Z., J.E.J., M.O., U.A., H.A. and T.T.N. contributed to the data set. H.Y.L. and X.Y.L. designed and conducted the analyses and wrote the manuscript. M.J.B., P.D. and M.S.E. edited portions of the manuscript. D.Z., B.W., H.N., S.Y., J.E.J., M.O., M.J.B., P.D., M.S.E., U.A. and H.A. provided critical comments on the manuscript.

CONFLICT OF INTEREST

The authors declare no competing interests.

FUNDING

This research was supported by the National Natural Science Foundation of China (No. 32130012, 31972871, 32370484), the 2115 Talent Development Program of China Agricultural University, the Science & Technology Fundamental Resources Investigation Program (Grant No. 2022FY202100), the Changjiang Scholars Program (2018), the Grant-in-Aid for JSPS Fellows (no. JP20J00159) from the Japan Society for the Promotion of Science (JSPS), Tokyo, Japan, and the National Animal Collection Resource Center, China. Hongyu Li was funded by China Scholarship Council (No. 202106350102).

REFERENCES

Abrams P. 1983. The theory of limiting similarity. Annu. Rev. Ecol. Evol. Syst., 14:359–376.

Abrams P.A. 2000. The evolution of predator-prey interactions: Theory and evidence. Annual Review of Ecology and Systematics, 31:79–105.

Alfaro M.E., Santini F., Brock C., Alamillo H., Dornburg A., Rabosky D.L., Carnevale G., Harmon L.J. 2009. Nine exceptional radiations plus high turnover explain species diversity in jawed vertebrates. Proc. Natl Acad. Sci. USA, 106:13410–13414.

Anderson M.J. 2001. A new method for non-parametric multivariate analysis of variance. Austral Ecology, 26:32–46.

Anker A., Ahyong S.T., Noel P.Y., Palmer A.R. 2006. Morphological phylogeny of alpheid shrimps: Parallel preadaptation and the origin of a key morphological innovation, the snapping claw. Evolution, 60:2507–2528.

Ardila-Camacho A., Martins C.C., Aspöck U., Contreras-Ramos A. 2021. Comparative morphology of extant raptorial Mantispoidea (Neuroptera: Mantispidae, Rhachiberothidae) suggests a non-monophyletic Mantispidae and a single origin of the raptorial condition within the superfamily. Zootaxa, 4992:1–89.

Aspöck H., Aspöck U., Hölzel H. 1980a. Die Neuropteren Europas. Vol. 1. Goecke and Evers, Krefeld, West Germany.

Aspöck H., Aspöck U., Hölzel H. 1980b. Die Neuropteren Europas. Vol. 2. Goecke and Evers, Krefeld, West Germany.

Aspöck U., Mansell M.W. 1994. A revision of the family Rhachiberothidae Tjeder, 1959, stat. n. (Neuroptera). Systematic Entomology, 19:181–206.

Aspöck U., Nemeschkal H.L. 1997. A cladistic analysis of the Berothidae (Neuroptera). Neuropterology 1997. Proceedings of the Sixth International Symposium on Neuropterology (13-16 July 1997, Helsinki, Finland). Acta Zoologica Fennica, 209:45–63.

Aspöck U., Randolf S. 2014. Beaded lacewings - a pictorial identification key to the genera, their biogeographics and a phylogentic analysis (Insecta: Neuroptera: Berothidae). Deutsche Entomologische Zeitschrift, 61:155–172.

Barido-Sottani J., Aguirre-Fernandez G., Hopkins M.J., Stadler T., Warnock R. 2019. Ignoring stratigraphic age uncertainty leads to erroneous estimates of species divergence times under the fossilized birth - death process. Proceedings of the Royal Society B: Biological Sciences, 286:20190685.

Bascompte J. 2009. Disentangling the web of life. Science, 325:416–419.

Benson R.B.J. 2018. Dinosaur Macroevolution and Macroecology. Annual Review of Ecology, Evolution, and Systematics, 49:379–408.

Benson R.B.J., Campione N.E., Carrano M.T., Mannion P.D., Sullivan C., Upchurch P., Evans D.C.

2014. Rates of dinosaur body mass evolution indicate 170 million years of sustained ecological innovation on the avian stem lineage. PLoS biology, 12:e1001853.

Benton M.J., Donoghue P.C.J. 2007. Paleontological evidence to date the tree of life. Molecular Biology and Evolution, 24:26–53.

Benton M.J., Wilf P., Sauquet H. 2022. The Angiosperm Terrestrial Revolution and the origins of modern biodiversity. New Phytologist, 233:2017–2035.

Blaimer B.B., Santos B.F., Cruaud A., Gates M.W., Kula R.R., Mikó I., Rasplus J.Y., Smith D.R., Talamas E.J., Brady S.G., Buffington M.L. 2023. Key innovations and the diversification of Hymenoptera. Nature Communications, 14:1212.

Burns J.H., Strauss S.Y. 2011. More closely related species are more ecologically similar in an experimental test. Proc. Natl Acad. Sci. USA, 108:5302–5307.

Castro-Huertas V., Forero D., Grazia J. 2019. Comparative morphology of the raptorial leg in thread-legged bugs of the tribe Metapterini Stal, 1859 (Hemiptera, Heteroptera, Reduviidae, Emesinae). Zoomorphology, 138:97–116.

Černý D., Madzia D., Slater G.J. 2021. Empirical and Methodological Challenges to the Model-Based Inference of Diversification Rates in Extinct Clades, 71:153–171.

Chan W.P. 1998. Visual input to the efferent control system of a fly's gyroscope (vol 280, pg 289, 1998). Science, 280:659–659.

Chase J.M., Leibold M.A. 2003. Ecological Niches: Linking Classical and Contemporary Approaches. University of Chicago Press.

Clarke R., Ressom H.W., Wang A.T., Xuan J.H., Liu M.C., Gehan E.A., Wang Y. 2008. The properties of high-dimensional data spaces: implications for exploring gene and protein expression data. Nature Reviews Cancer, 8:37–49.

Clavel J., Julliard R., Devictor V. 2011. Worldwide decline of specialist species: toward a global functional homogenization? Frontiers in Ecology and the Environment, 9:222–228.

Condamine F.L., Clapham M.E., Kergoat G.J. 2016. Global patterns of insect diversification: Towards a reconciliation of fossil and molecular evidence? Scientific Reports, 6:19208.

Condamine F.L., Nel A., Grandcolas P., Legendre F. 2020. Fossil and phylogenetic analyses reveal recurrent periods of diversification and extinction in dictyopteran insects. Cladistics, 36:394–412.

Corso J.D., Bernardi M., Sun Y., Song H., Seyfullah L.J., Preto N., Gianolla P., Ruffell A., Kustatscher E., Roghi G., Merico A., Hohn S., Schmidt A.R., Marzoli A., Newton R.J., Wignall P.B., Benton M.J. 2020. Extinction and dawn of the modern world in the Carnian (Late Triassic). Science Advances, 6:eaba0099.

Creel S., Christianson D. 2008. Relationships between direct predation and risk effects. Trends in Ecology & Evolution, 23:194–201.

Day T., Young K.A. 2004. Competitive and Facilitative Evolutionary Diversification. BioScience, 54:101–109.

Devetak D., Klokocovnik V. 2016. The feeding biology of adult lacewings (Neuroptera): A review. Trends in Entomology, 12:29–42.

Dixon P. 2003. VEGAN, a package of R functions for community ecology. Journal of Vegetation Science, 14:927–930.

Donoghue P.C.J., Benton M.J. 2007. Rocks and clocks: calibrating the Tree of Life using fossils and molecules. Trends in Ecology & Evolution, 22:424–431.

Drury J.P., Tobias J.A., Kevin J. Burns, Mason N.A., Shultz A.J., Morlon H. 2018. Contrasting impacts of competition on ecological and social trait evolution in songbirds. Plos Biology, 16:e2003563.

Dudley R. 2000. The biomechanics of insect flight: form, function, evolution.

Emlen D.J. 2001. Costs and the diversification of exaggerated animal structures. Science, 291:1534–1536.

Engel M.S., Winterton S.L., Breitkreuz L.C.V. 2018. Phylogeny and Evolution of Neuropterida: Where Have Wings of Lace Taken Us? Annual Review of Entomology, 63:531–551.

Erwin D.H. 1994. The Permo-Triassic extinction. Nature, 367:231–236.

Erwin D.H. 2015. Novelty and innovation in the history of life. Current Biology, 25:R930–R940.

Fabreti L.G., Hoehna S. 2022. Convergence assessment for Bayesian phylogenetic analysis using MCMC simulation. Methods in Ecology and Evolution, 13:77–90.

Faruque I., Humbert J.S. 2010. Dipteran insect flight dynamics. Part 1 Longitudinal motion about hover. Journal of Theoretical Biology, 264:538–552.

Fisher D.C. 2008. Stratocladistics: integrating temporal data and character data in phylogenetic inference. Annual Review of Ecology Evolution and Systematics, 39:365–385.

Forkner R.M., Dahl J., Fildani A., Barbanti S.M., I.A.Yurchenko, Moldowan J.M. 2021. Anatomy of an extinction revealed by molecular fossils spanning OAE2. Scientific Reports, 11:13621.

Futuyma D.J., Moreno G. 1988. The evolution of ecological specialization. Annual Review of Ecology and Systematics, 19:207–233.

Gavryushkina A., Welch D., Stadler T., Drummond A.J. 2014. Bayesian Inference of Sampled Ancestor Trees for Epidemiology and Fossil Calibration. Plos Computational Biology, 10:e1003919.

Gavryushkina A., Zhang C. 2020. Total-evidence dating and the fossilized birth–death model.

Gianoli E. 2004. Evolution of a climbing habit promotes diversification in flowering plants. Proceedings of the Royal Society B-Biological Sciences, 271:2011–2015.

Goloboff P.A., Catalano S.A. 2016. TNT version 1.5, including a full implementation of phylogenetic morphometrics. Cladistics, 32:221–238.

Gonzalez A., Loreau M. 2009. The Causes and Consequences of Compensatory Dynamics in Ecological Communities. Annual Review of Ecology Evolution and Systematics, 40:393–414.

Gould S.J., Eldredge N. 1977. Punctuated equilibria: the tempo and mode of evolution reconsidered. Paleobiology, 3(2):115–151.

Grant P.R., Grant B.R. 2006. Evolution of Character Displacement in Darwin's Finches. Science, 313:224–226.

Griffin J.N., Byrnes J.E.K., Cardinale B.J. 2013. Effects of predator richness on prey suppression: a meta-analysis. Ecology, 94:2180–2187.

Grimaldi D.A., Engel M.S., Nascimbene P.C. 2002. Fossiliferous cretaceous amber from Myanmar (Burma): Its rediscovery, biotic diversity, and paleontological significance. American Museum Novitates:1–72.

Hautmann M. 2012. Extinction: End-Triassic Mass Extinction. Encyclopedia of Life Sciences:1–10.

Heard S.B., Hauser D.L. 1995. Key evolutionary innovations and their ecological mechanisms. Hist. Biol., 10:151–173.

Höhna S., Stadler T., Ronquist F., Britton T. 2011. Inferring speciation and extinction rates under different sampling schemes. Molecular Biology and Evolution, 28:2577–2589.

Holt R.D. 2009. Bringing the Hutchinsonian niche into the 21st century: Ecological and evolutionary

perspectives. Proceedings of the National Academy of Sciences of the United States of America, 106:19659–19665.

Hopkins M., Gerber S. 2017. Evolutionary developmental biology. Springer, Cham.

Hopkins M.J., St John K. 2018. A new family of dissimilarity metrics for discrete character matrices that include inapplicable characters and its importance for disparity studies. Proceedings of the Royal Society B: Biological Sciences, 285:2018178.

Hull P. 2015. Life in the aftermath of mass extinctions. Current Biology, 25:R941–R952.

Hunter J.P. 1998. Key innovations and the ecology of macroevolution. Trends in Ecology & Evolution, 13:31–36.

Jouault C., Legendre F., Grandcolas P., Nel A. 2021. Revising dating estimates and the antiquity of eusociality in termites using the fossilized birth-death process. Systematic Entomology, 46:592–610.

Jouault C., Nel A., Legendre F., Condamine F.L. 2022a. Estimating the drivers of diversification of stoneflies through time and the limits of their fossil record. Insect Systematics and Diversity, 6:4.

Jouault C., Nel A., Perrichot V., Legendre F., Condamine F.L. 2022b. Multiple drivers and lineage-specific insect extinctions during the Permo-Triassic. Nature Communications, 13:7512.

Kalyaanamoorthy S., Bui Quang M., Wong T.K.F., von Haeseler A., Jermiin L.S. 2017. ModelFinder: fast model selection for accurate phylogenetic estimates. Nature Methods, 14:587–589.

Kania I., Wang B., Szwedo J. 2015. *Dicranoptycha* Osten Sacken, 1860 (Diptera, Limoniidae) from the earliest Cenomanian Burmese amber. Cretaceous Research, 52:522–530.

Kass R.E., Raftery A.E. 1995. Bayes factors. Journal of the American Statistical Association, 90:773–795.

Khramov A.V. 2023. The first Triassic beaded lacewing (Neuroptera: Berothidae) from Central Asia, with redescription of *Mesoberotha superba* (Riek, 1955). Zootaxa, 5330:287–294.

King B. 2021. Bayesian tip-dated phylogenetics in paleontology: topological effects and stratigraphic fit. Systematic Biology, 70:283–294.

King B., Qiao T., Lee M.S.Y., Zhu M., Long J.A. 2017. Bayesian morphological clock methods resurrect placoderm monophyly and reveal rapid early evolution in jawed vertebrates. Systematic Biology, 66:499–516.

Kingsolver J.G., Pfennig D.W. 2007. Patterns and power of phenotypic selection in nature. Bioscience, 57:561–572.

Klein C.G., Pisani D., Field D.J., Lakin R., Wills M.A., Longrich N.R. 2021. Evolution and dispersal of snakes across the Cretaceous-Paleogene mass extinction. nature Communications, 12:5335.

Korn D., Hopkins M.J., Walton S.A. 2013. Extinction space--a method for the quantification and classification of changes in morphospace across extinction boundaries. Evolution, 67:2795–2810.

Kral K. 2013. Vision in the mantispid: a sit-and-wait and stalking predatory insect. Physiological Entomology, 38:1–12.

Krishna S., Cho M., Wehmann H.-N., Engels T., Lehmann F.-O. 2020. Wing design in flies: properties and aerodynamic function. Insects, 11:466.

Lai D., Chen P., Li S., Xiang X., Ou H., Kang N., Yang J., Pang H., Shih C., Labandeira C.C., Ren D., Yang Q., Shi C. 2023. The associated evolution of raptorial foreleg and mantispid diversification during 200 million years. National science review, 10:278–278.

Lambkin K.J. 1986a. A revision of the Australian Mantispidae (Insecta: Neuroptera) with a contribution to the classification of the family. I. General and Drepanicinae. Australian Journal of Zoology, Supplementary Series, 34:1–142.

Lambkin K.J. 1986b. A revision of the Australian Mantispidae (Insecta: Neuroptera) with a contribution to the classification of the family. II. Calomantispinae and Mantispinae. Australian Journal of Zoology, Supplementary Series, 34:1–113.

Lamsdell J.C., Stein M., Selden P.A. 2013. Kodymirus and the case for convergence of raptorial appendages in Cambrian arthropods. Naturwissenschaften, 100:811–825.

Le Bagousse-Pinguet Y., Soliveres S., Gross N., Torices R., Berdugo M., Maestre F.T. 2019. Phylogenetic, functional, and taxonomic richness have both positive and negative effects on ecosystem multifunctionality. Proceedings of the National Academy of Sciences of the United States of America, 116:8419–8424.

Lehtonen S., Silvestro D., Karger D.N., Scotese C., Tuomisto H., Kessler M., Pena C., Wahlberg N., Antonelli A. 2017. Environmentally driven extinction and opportunistic origination explain fern diversification patterns. Scientific Reports, 7:4831.

Lepage T., Bryant D., Philippe H., Lartillot N. 2007. A general comparison of relaxed molecular clock models. Molecular Biology and Evolution, 24:2669–2680.

Lerosey-Aubril R., Pates S. 2018. New suspension-feeding radiodont suggests evolution of microplanktivory in Cambrian macronekton. Nature Communications, 9:3774.

Levis N.A., Isdaner A.J., Pfennig D.W. 2018. Morphological novelty emerges from pre-existing phenotypic plasticity. Nature Ecology & Evolution, 2:1289–1297.

Lewis P.O. 2001. A likelihood approach to estimating phylogeny from discrete morphological character data. Systematic Biology, 50:913–925.

Li D., Aspöck H., Aspöck U., Liu X.Y. 2020. New beaded lacewings (Insecta: Neuroptera: Berothidae) from Indochina. Zootaxa, 4890:509–520.

Li H.Y., Zhuo D., Cao L.R., Wang B., Poinar G., Ohl M., Liu X.Y. 2022. New cretaceous fossil mantispids highlight the palaeodiversity of the extinct subfamily Doratomantispinae (Neuroptera: Mantispidae) Organisms Diversity & Evolution, 22:731–731.

Li H.Y., Zhuo D., Wang B., Nakamine H., Yamamoto S., Zhang W.W., Ling J.N., Ohl M., Aspöck U., Aspöck H., Liu X.Y. 2023. New genera and species of Mantispoidea (Insecta, Neuroptera) from the mid-Cretaceous Kachin amber, northern Myanmar. Palaeoentomology, 006:549–611.

Liu X.Y., Winterton S.L., Wu C., Piper R., Ohl M. 2015. A new genus of mantidflies discovered in the Oriental region, with a higher-level phylogeny of Mantispidae (Neuroptera) using DNA sequences and morphology. Systematic Entomology, 40:183–206.

Lloyd G., Ruta M., Tarver J., Benton M. 2008. Dinosaurs and the cretaceous terrestrial revolution. Journal of Vertebrate Paleontology, 28:107A–107A.

Lloyd G.T. 2016. Estimating morphological diversity and tempo with discrete character-taxon matrices: implementation, challenges, progress, and future directions. Biological Journal of the Linnean Society, 118:131–151.

Lloyd G.T. 2018. Journeys through discrete-character morphospace: synthesizing phylogeny, tempo, and disparity. Palaeontology, 61:637–645.

Lloyd G.T., Wang S.C., Brusatte S.L. 2012. Identifying heterogeneity in rates of morphological evolution: Discrete character change in the evolution of lungfish (Sarcopterygii, Dipnoi). Evolution, 66:330–348.

Lu J., Zhang P.X., Dal Corso J., Yang M.F., Wignall P.B., Greene S.E., Shao L.Y., Lyu D., Hilton J. 2021. Volcanically driven lacustrine ecosystem changes during the Carnian Pluvial Episode (Late Triassic). Proceedings of the National Academy of Sciences of the United States of America, 118:e2109895118.

Lu X.M., Liu X.Y. 2021. The Neuropterida from the mid-Cretaceous of Myanmar: A spectacular palaeodiversity bridging the Mesozoic and present faunas. Cretaceous Research, 121:104727.

Lu X.M., Wang B., Zhang W.W., Ohl M., Engel M.S., Liu X.Y. 2020. Cretaceous diversity and disparity in a lacewing lineage of predators (Neuroptera: Mantispidae). Proceedings of the Royal Society B: Biological Sciences, 287:20200629.

Lynch M., Conery J.S. 2000. The evolutionary fate and consequences of duplicate genes. Science, 290:1151–1155.

Makarkin V.N., Yang Q., Reng D. 2011. Two new species of *Sinosmylites* Hong (Neuroptera, Berothidae) from the Middle Jurassic of China, with notes on Mesoberothidae. Zookeys:199–215.

Maliet O., Hartig F., Morlon H. 2019. A model with many small shifts for estimating species-specific diversification rates. Nature Ecology & Evolution, 3:1086–1092.

Marki P.Z., Kennedy J.D., Cooney C.R., Rahbek C., Fjeldså J. 2019. Adaptive radiation and the evolution of nectarivory in a large songbird clade. Evolution, 73:1226–1240.

Martynova O.M. 1958. Novye nasekomye iz Permskikh i Mezozoiskikh otlozhenii SSSR [=New insects from the Permian and Mesozoic deposits of the USSR]. Materialy k Osnovam Paleontologii, 2:69–94.

Matzke N.J., Irmis R.B. 2018. Including autapomorphies is important for paleontological tip-dating with clocklike data, but not with non-clock data. Peerj, 6:e4553.

McCann K.S. 2000. The diversity-stability debate. Nature, 405:228–233.

McGee M.D., Borstein S.R., Neches R.Y., Buescher H.H., Seehausen O., Wainwright P.C. 2015. A pharyngeal jaw evolutionary innovation facilitated extinction in Lake Victoria cichlids. Science, 350:1077–1079.

McGill B.J., Enquist B.J., Weiher E., Westoby M. 2006. Rebuilding community ecology from functional traits. Trends in Ecology & Evolution, 21:178–185.

McKinney M.L. 1997. Extinction vulnerability and selectivity: Combining ecological and paleontological views. Annual Review of Ecology and Systematics, 28:495–516.

Meyers S.R., Siewert S.E., Singer B.S., Sageman B.B., Condon D.J., Obradovich J.D., Jicha B.R., Sawyer D.A. 2012. Intercalibration of radioisotopic and astrochronologic time scales for the Cenomanian-Turonian boundary interval, Western Interior Basin, USA. Geology, 40:7–10.

Miller A.H., Stroud J.T., Losos J.B. 2023. The ecology and evolution of key innovations. Trends in Ecology & Evolution, 38:122–131.

Mitchell J.S., Etienne R.S., Rabosky D.L. 2018. Inferring Diversification Rate Variation From Phylogenies With Fossils. Systematic Biology, 68:1–18.

Moysiuk J., Caron J.-B. 2021. Exceptional multifunctionality in the feeding apparatus of a mid-Cambrian radiodont. Paleobiology, 47:704–724.

Nakamine H., Yamamoto S., Takahashi Y. 2020. Hidden diversity of small predators: new thorny lacewings from mid-Cretaceous amber from northern Myanmar (Neuroptera: Rhachiberothidae: Paraberothinae). Geological Magazine, 157:1149–1175.

Nguyen L.T., Schmidt H.A., von Haeseler A., Minh B.Q. 2015. IQ-TREE: A Fast and Effective

Stochastic Algorithm for Estimating Maximum-Likelihood Phylogenies. Molecular Biology and Evolution, 32:268–274.

Nicholson D.B., Ross A.J., Mayhew P.J. 2014. Fossil evidence for key innovations in the evolution of insect diversity. Proceedings of the Royal Society B-Biological Sciences, 281:20141823.

Nylander J.A.A., Ronquist F., Huelsenbeck J.P., Nieves-Aldrey J. 2004. Bayesian Phylogenetic Analysis of Combined Data. Systematic Biology, 53:47–67.

Oswald J.D. 2022. Neuropterida Species of the World. Lacewing Digital Library.

Oufiero C.E. 2020. Evolutionary diversification in the raptorial forelegs of Mantodea: Relations to body size and depth perception. Journal of Morphology, 281:513–522.

Paine R.T. 1966. Food web complexity and species diversity. American Naturalist, 100:65–75.

Pangle K.L., Peacor S.D., Johannsson O.E. 2007. Large nonlethal effects of an invasive invertebrate predator on zooplankton population growth rate. Ecology, 88:402–412.

Pastore A.I., Barabás G., Bimler M.D., Mayfield M.M., Miller T.E. 2021. The evolution of niche overlap and competitive differences. Nature Ecology & Evolution, 5:330–337.

Pearce M.A., Jarvis I., Tocher B.A. 2009. The Cenomanian–Turonian boundary event, OAE2 and palaeoenvironmental change in epicontinental seas: New insights from the dinocyst and geochemical records. Palaeogeography, Palaeoclimatology, Palaeoecology, 280: 207–234.

Pérez-de la Fuente R., Peñalver E. 2019. A mantidfly in Cretaceous Spanish amber provides insights into the evolution of integumentary specialisations on the raptorial foreleg. Scientific Reports, 9:1–16.

Peris D., Condamine F.L. 2024. The angiosperm radiation played a dual role in the diversification of insects and insect pollinators. Nature Communications, 15:552.

Petchey O.L., Gaston K.J. 2002. Functional diversity (FD), species richness and community composition. Ecology Letters, 5:402–411.

Poivre C. 1974. La patte prothoracique des Mantispidés et ses récepteurs sensoriels fémoraux. Bulletin du Muséum national d'histoire naturelle, 261:1633–1647.

Poivre C. 1978. Morphologie externe comparée de *Gerstaeckerella gigantea* Enderlein [Planipennia, Mantispidae]. Annales de la Société Entomologique de France (N.S.), 14:191–206.

Porter M.L., Zhang Y.F., Desai S., Caldwell R.L., Cronin T.W. 2010. Evolution of anatomical and physiological specialization in the compound eyes of stomatopod crustaceans. Journal of Experimental Biology, 213:3473–3486.

Rabosky D.L. 2014. Automatic detection of key innovations, rate shifts, and diversity-dependence on phylogenetic trees. Plos One, 9:e89543.

Rabosky D.L. 2017. Phylogenetic tests for evolutionary innovation: the problematic link between key innovations and exceptional diversification. Philosophical Transactions of the Royal Society B-Biological Sciences, 372:20160417.

Rambaut A., Drummond A.J., Xie D., Baele G., Suchard M.A. 2018. Posterior summarization in Bayesian phylogenetics using Tracer 1.7. Systematic Biology, 67:901–904.

Ronquist F., Teslenko M., van der Mark P., Ayres D.L., Darling A., Hohna S., Larget B., Liu L., Suchard M.A., Huelsenbeck J.P. 2012. MrBayes 3.2: Efficient Bayesian Phylogenetic Inference and Model Choice Across a Large Model Space. Systematic Biology, 61:539–542.

Roquet C., Boucher F.C., Thuiller W., Lavergne S. 2013. Replicated radiations of the alpine genus *Androsace* (Primulaceae) driven by range expansion and convergent key innovations. Journal of Biogeography, 40:1874–1886.

Roy C.L., Roux C., Authier E., Parrinello H., Bastide H., Debat V., Llaurens V. 2021. Convergent morphology and divergent phenology promote the coexistence of Morpho butterfly species. Nature Communications, 12:7248.

Schluter D. 2000. The Ecology of Adaptive Radiation. Oxford University Press.

Schmidt M., Melzer R.R., Bicknell R.D.C. 2022. Kinematics of whip spider pedipalps: A 3D comparative morpho-functional approach. Integrative Zoology, 17:156–167.

Shi G., Grimaldi D.A., Harlow G.E., Wang J., Wang J., Yang M., Lei W., Li Q., Li X. 2012. Age constraint on Burmese amber based on U-Pb dating of zircons. Cretaceous Research, 37:155–163.

Silvestro D., Antonelli A., Salamin N., Quental T.B. 2015a. The role of clade competition in the diversification of North American canids. Proceedings of the National Academy of Sciences of the United States of America, 112:8684–8689.

Silvestro D., Cascales-Minana B., Bacon C.D., Antonelli A. 2015b. Revisiting the origin and diversification of vascular plants through a comprehensive Bayesian analysis of the fossil record. New Phytologist, 207:425–436.

Simoes T.R., Caldwell M.W., Pierce S.E. 2020a. Sphenodontian phylogeny and the impact of model choice in Bayesian morphological clock estimates of divergence times and evolutionary rates. Bmc Biology, 18:191.

Simoes T.R., Vernygora O., Caldwell M.W., Pierce S.E. 2020b. Megaevolutionary dynamics and the timing of evolutionary innovation in reptiles. Nature Communications, 11:3322.

Simpson G.G. 1953. The Major Features of Evolution. New York, Columbia Univ. Press.

Smith D.M., Marcot J.D. 2015. The fossil record and macroevolutionary history of the beetles. Proceedings of the Royal Society B-Biological Sciences, 282:20150060.

Snedden J.W., Liu C. 2010. A compilation of Phanerozoic sea-level change, coastal onlaps and recommended sequence designations. Search and Discovery Article:40594.

Sperling E.A., Frieder C.A., Raman A.V., Girguis P.R., Levin L.A., Knoll A.H. 2013. Oxygen, ecology, and the Cambrian radiation of animals. Proceedings of the National Academy of Sciences of the United States of America, 110 (33):13446–13451.

Stroud J.T., Losos J.B. 2016. Ecological opportunity and adaptive radiation. Annual Review of Ecology, Evolution, and Systematics, 47:507–532.

Sutherland J.T.F., Moon B.C., Stubbs T.L., Benton M.J. 2019. Does exceptional preservation distort our view of disparity in the fossil record? Proceedings of the Royal Society B: Biological Sciences, 286:20190091.

Terborgh J.W. 2015. Toward a trophic theory of species diversity. Proceedings of the National Academy of Sciences of the United States of America, 112:11415–11422.

Thorne J.L., Kishino H. 2002. Divergence time and evolutionary rate estimation with multilocus data. Systematic Biology, 51:689–702.

Tilman D. 1999. The ecological consequences of changes in biodiversity: A search for general principles. Ecology, 80:1455–1474.

Turner A.H., Pritchard A.C., Matzke N.J. 2017. Empirical and Bayesian approaches to fossil only divergence times: A study across three reptile clades. Plos One, 12:e0169885.

Vannier J., Garcia-Bellido D.C., Hu S.X., Chen A.L. 2009. Arthropod visual predators in the early pelagic ecosystem: evidence from the Burgess Shale and Chengjiang biotas. Proceedings of the Royal Society B: Biological Sciences, 276:2567–2574.

Vasilikopoulos A., Misof B., Meusemann K., Lieberz D., Flouri T., Beutel R.G., Niehuis O., Wappler T., Rust J., Peters R.S., Donath A., Podsiadlowski L., Mayer C., Bartel D., Boehm A., Liu S., Kapli P., Greve C., Jepson J.E., Liu X., Zhou X., Aspoeck H., Aspoeck U. 2020. An integrative phylogenomic approach to elucidate the evolutionary history and divergence times of Neuropterida (Insecta: Holometabola). Bmc Evolutionary Biology, 20:64.

Verleysen M., Francois D. 2005. The curse of dimensionality in data mining and time series prediction. Computational Intelligence and Bioinspired Systems, Proceedings, 3512:758–770.

Vermeij G.J. 2001. Innovation and evolution at the edge: origins and fates of gastropods with a labral tooth. Biological Journal of the Linnean Society, 72:461–508.

Wang K.J., Yan X.H., Chen L.F. 2011. Geometric double-entity model for recognizing far-near relations of clusters. Science China-Information Sciences, 54:2040–2050.

Wang Y.Y., Liu X.Y., Garzon-Orduna I.J., Winterton S.L., Yan Y., Aspoeck U., Aspoeck H., Yang D. 2017. Mitochondrial phylogenomics illuminates the evolutionary history of Neuropterida. Cladistics, 33:617–636.

Weirauch C., Forero D., Jacobs D.H. 2011. On the evolution of raptorial legs - an insect example (Hemiptera: Reduviidae: Phymatinae). Cladistics, 27:138–149.

Wieland F. 2013. The phylogenetic system of Mantodea (Insecta: Dictyoptera). Georg-August-Universität Göttingen, p. 222.

Wignall P.B. 2001. Large igneous provinces and mass extinctions. Earth-Science Reviews, 53:1–33.

Willmann R. 1990. The phylogenetic position of the Rhachiberothinae and the basal sister-group relationships within the Mantispidae (Neuroptera). Systematic Entomology, 15:253–265.

Wills M.A., Briggs D.E.G., Fortey R.A. 1994. Disparity as an evolutionary index - a comparison of cambrian and recent arthropods. Paleobiology, 20:93–130.

Winterton S.L., Lemmon A.R., Gillung J.P., Garzon I.J., Badano D., Bakkes D.K., Breitkreuz L.C.V., Engel M.S., Lemmon E.M., Liu X., Machado R.J.P., Skevington J.H., Oswald J.D. 2018. Evolution of lacewings and allied orders using anchored phylogenomics (Neuroptera, Megaloptera, Raphidioptera). Systematic Entomology, 43:330–354.

Xie W., Lewis P.O., Fan Y., Kuo L., Chen M.H. 2011. Improving marginal likelihood estimation for Bayesian phylogenetic model selection. Systematic Biology, 60:150–160.

Yin Z.W., Lu L., Yamamoto S., Thayer M.K., Newton A.F., Cai C.Y. 2021. Dasycerine rove beetles: Cretaceous diversification, phylogeny and historical biogeography (Coleoptera: Staphylinidae: Dasycerinae). Cladistics, 37:185–210.

Yu Y.L., Zhang C., Xu X. 2021. Deep time diversity and the early radiations of birds. Proceedings of the National Academy of Sciences of the United States of America, 118:e2019865118.

Yu Y.L., Zhang C., Xu X. 2023. Complex macroevolution of pterosaurs. Current Biology, 33:770–779.

Zhang C., Stadler T., Klopfstein S., Heath T.A., Ronquist F. 2016. Total-evidence dating under the fossilized birth-death process. Systematic Biology, 65:228–249.

Zhang C., Wang M. 2019. Bayesian tip dating reveals heterogeneous morphological clocks in Mesozoic birds. Royal Society Open Science, 6:182062.

Figures

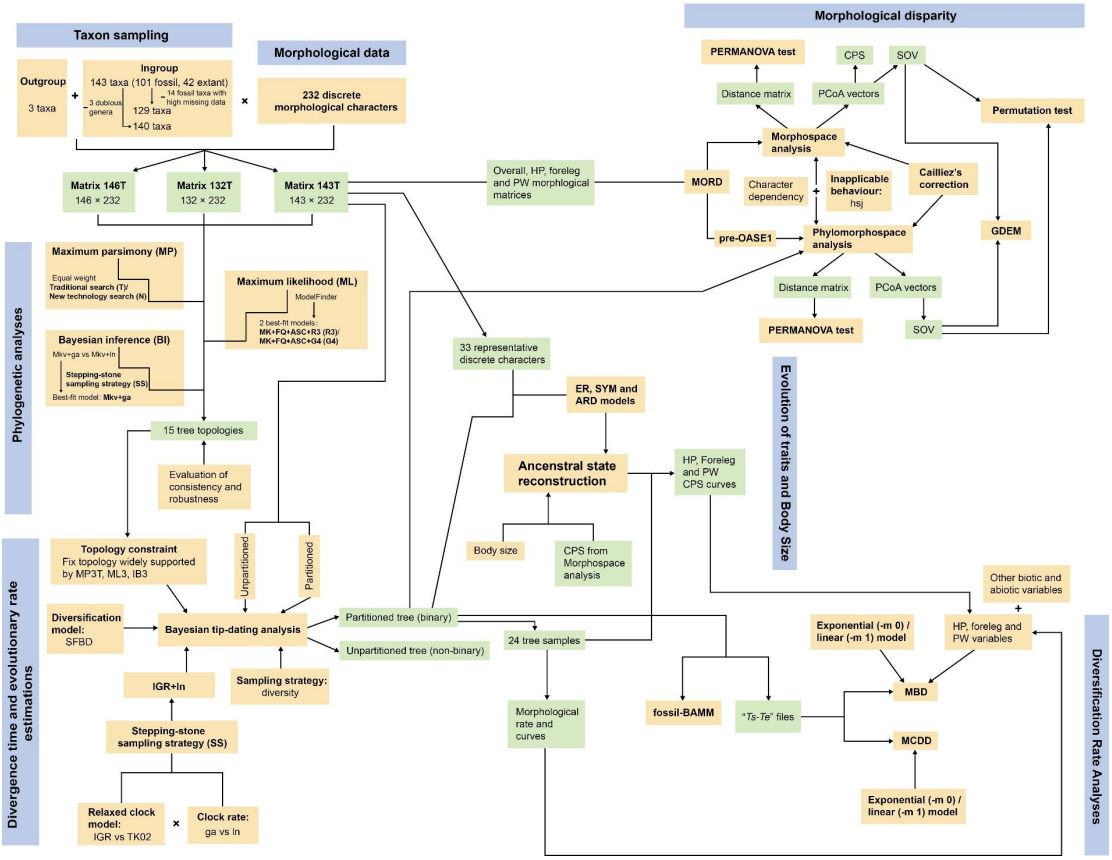

Figure 1. Pipeline of macroevolutionary analysis for Mantispoidea. Abbreviations: ARD, All-rates-different model; CPS, Comprehensive PCoA scores; ER, Equal-rates model; ga, Gamma distribution; GDEM, Geometric double-entity model; HP, Head & prothorax; IB3, Bayesian inference for matrix 143T (143×232); IGR, Independent gamma rates uncorrelated clock model; ln, Lognormal distribution; MBD, multivariate birth-death model; MCDD, multiple clade diversity dependence model; ML3, Maximum likelihood analysis for matrix 143T (143×232); MORD, Maximum observable rescaled distance; MP3T, Maximum parsimony analysis for matrix 143T (143×232) using traditional search; PCoA, Principal coordinate analysis PW, Pterothorax & wings; SFBD, Skyline fossilized birth-death model; TK02, Thorne and Kishino continuous autocorrelated clock model; SOV, Sum of variances; SYM, Symmetrical model.

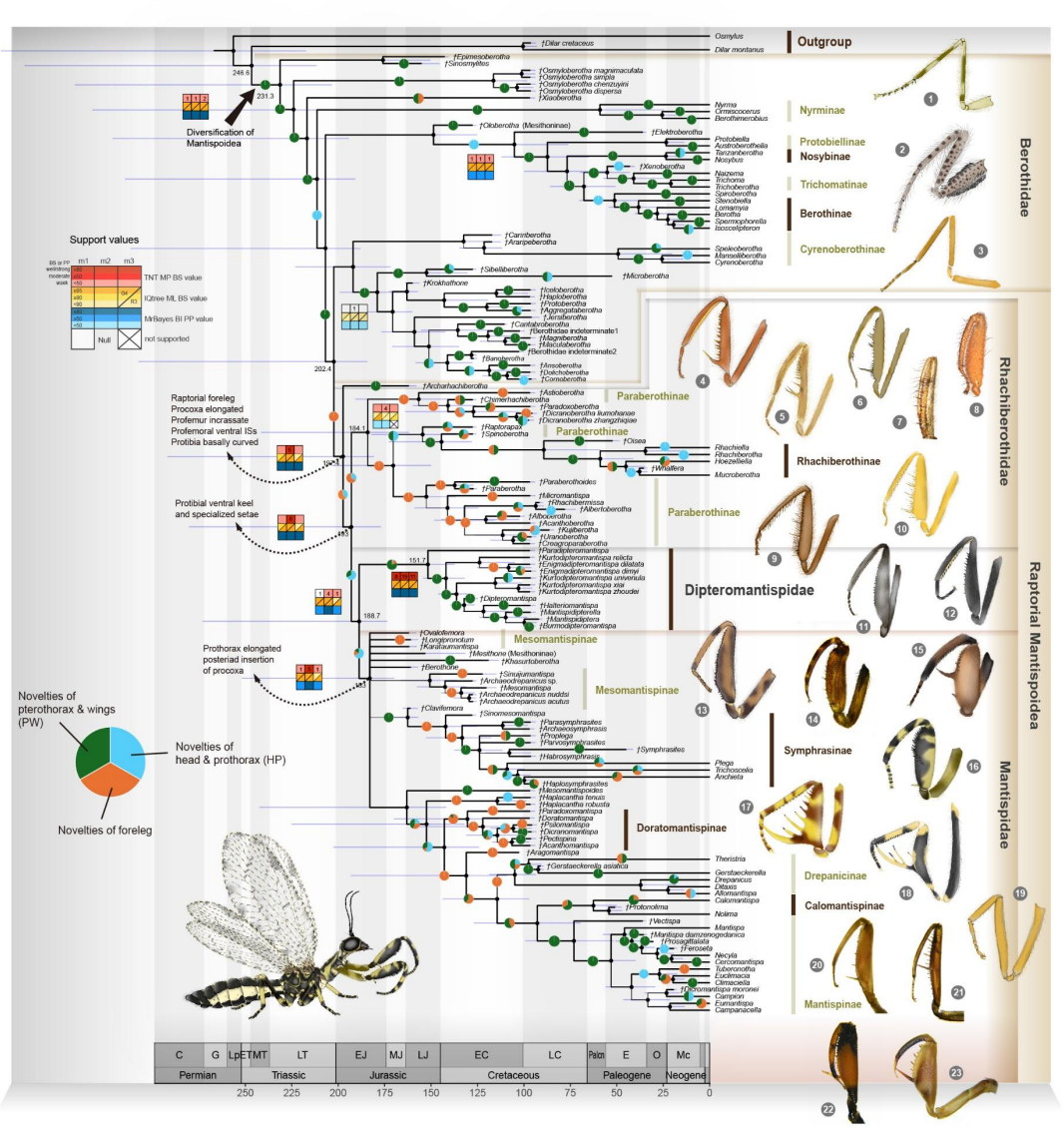

Figure 2. Time tree of Mantispoidea inferred by unpartitioned tip-dating Bayesian analysis based on morphological matrix 143T (232 × 143). Posterior median ages are mapped above each node. Dashed arrows indicate the unique synapomorphies of the major clades of raptorial Mantispoidea. Error bars (in violet) denote the 95% HPD intervals of age estimates. Squares with different colors at nodes represent the support value from different morphological matrices and analytical methods (The detailed interpretation of the squares is shown in the top-left illustration). The number in the square of MP analysis refers to the Bremer value. The pie charts display the proportion of novelties of different partitions. Left bottom: Reconstructed habitus of Cretaceous mantidfly †*Haplacantha robusta*. Forelegs of different mantispoid lineages are shown on the right: Berothidae: (1) †*Osmyloberotha*, (2) *Podallea*, (3) †*Haploberotha*; Rhachiberothidae: (4) †*Paradoxoberotha*, (5) †*Dicranoberotha*, (6) †*Astioberotha*, (7) *Rhachiberotha* (Ardila-Camacho et al. (2021): Fig. 21b), (8) *Mucroberotha* (Ardila-Camacho et al. (2021): Fig. 21a), (9) †*Paraberothoides*, (10) †*Creagroparaberotha*; †Dipteromantispidae: (11) †*Kurtodipteromantispa*, (12) †*Enigmadipteromantispa*; Mantispidae: (13) †*Archaeodrepanicus*, (14) *Plega*, (15) †*Mesomantispoides*, (16) †*Haplacantha*, (17) †*Doratomantispa*, (18) †*Acanthomantispa*, (19)

†*Psilomantispa*, (20) *Ditaxis*, (21) *Theristria*, (22) *Calomantispa*, (23) *Tuberonotha*

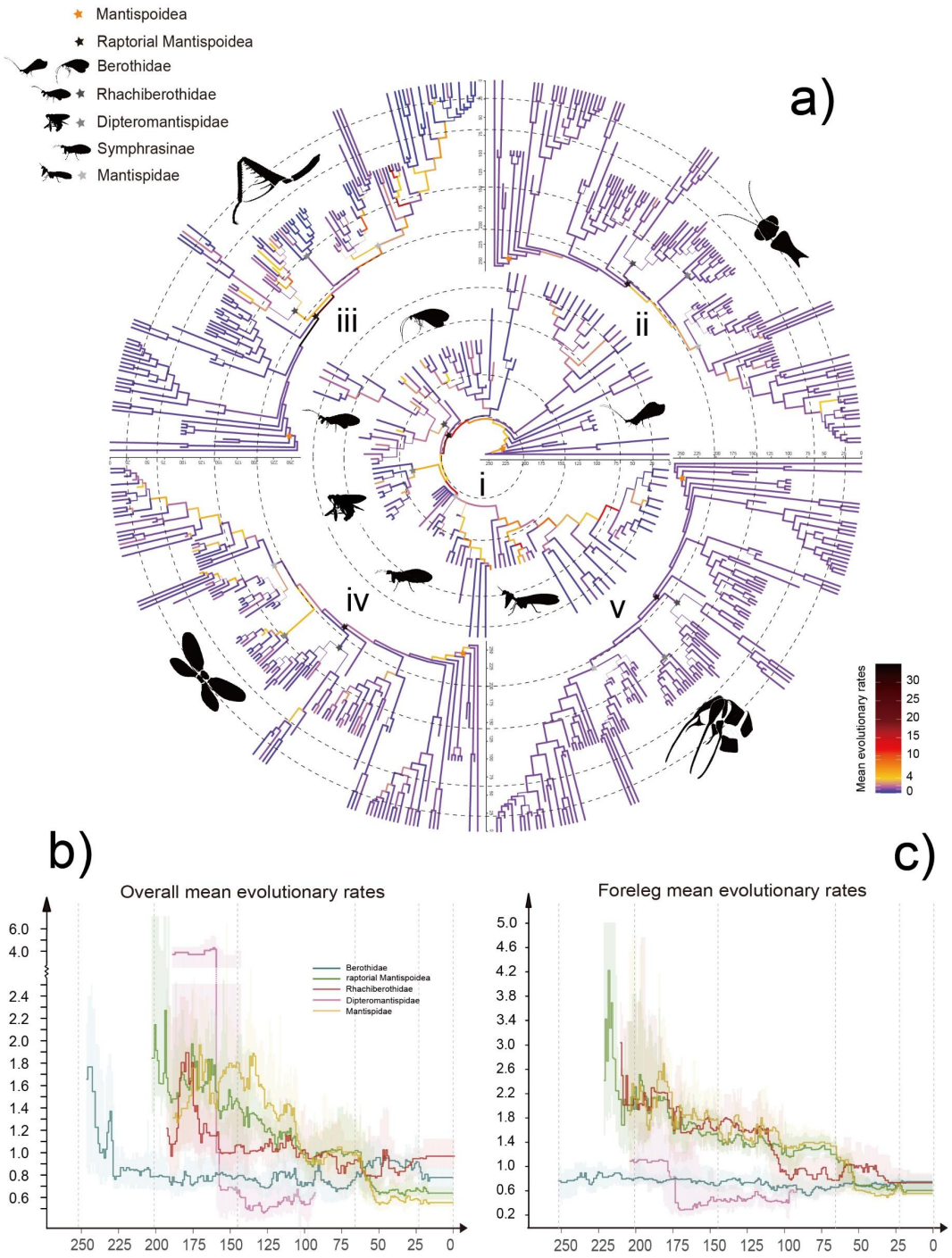

Figure 3. Morphological evolutionary rates of Mantispoidea. (a) Morphological mean evolutionary rates mapped on dated phylogenetic trees: i, Unpartitioned morphological rate tree; ii-v, Partitioned morphological rate tree; ii, HP rate tree; iii, Foreleg rate tree; iv, PW rate tree; v, Genitalia rate tree. Color of branches represents the mean relative clock rate along them. (b) Overall and (c) Foreleg mean morphological evolutionary rates of Berothidae, raptorial Mantispoidea, Rhachiberothidae and Mantispidae through time, estimated by unpartitioned and partitioned tip-dating Bayesian inference.

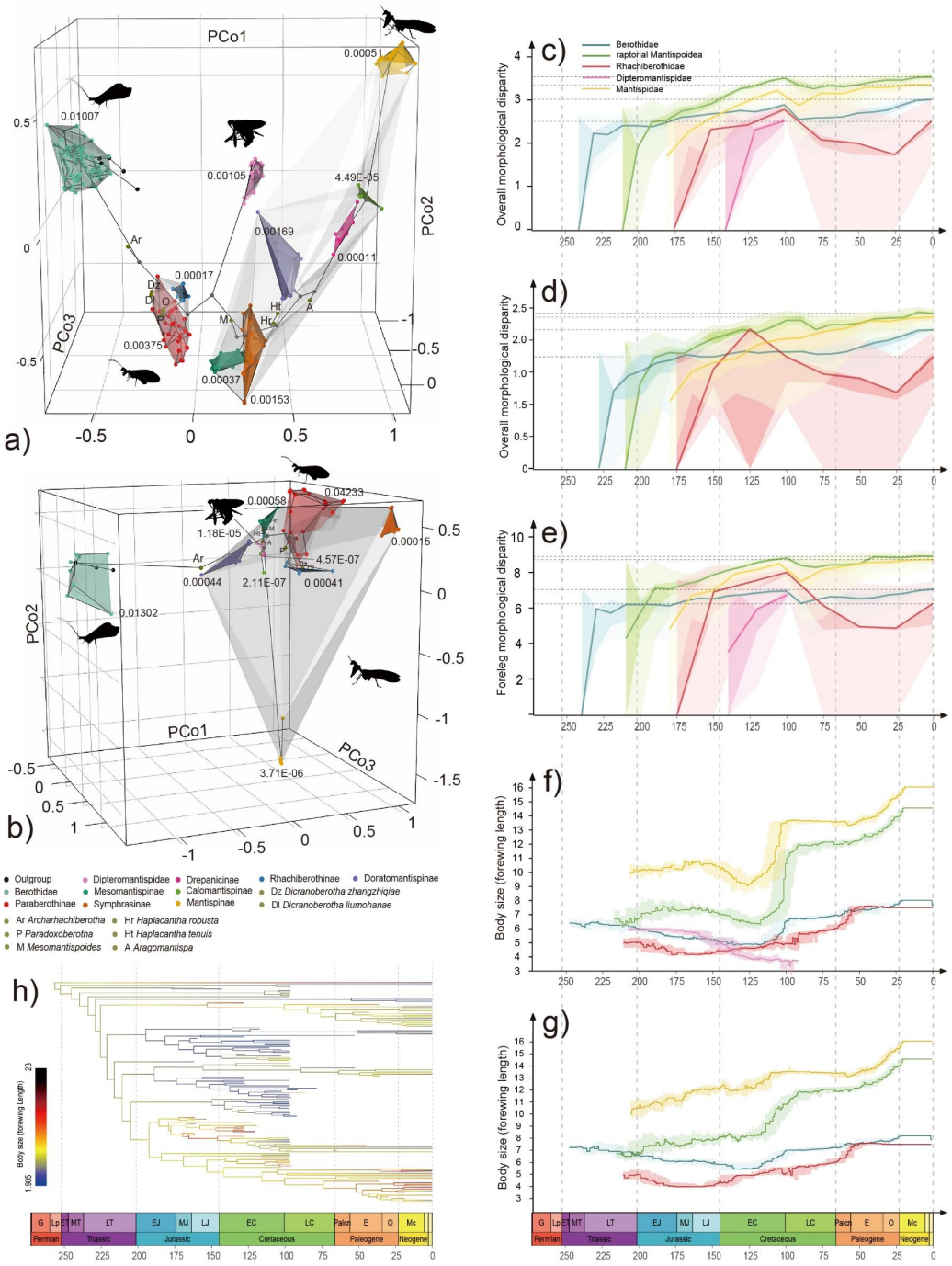

Figure 4. Morphological disparity and body size evolution of Mantispoidea. (a) Whole body and (b) Foreleg phylomorphospace 3D-plots (see the interactive 3D graphics on Dryad at https://doi.org/10.5061/dryad.h18931zth). The number on each 3D convex hull indicates its volume

value (see details in Supplementary Table 4). Whole body disparity in major mantispoid lineages through time, proxied by sum of variances, (c) including samples from the mid-Cretaceous of Myanmar, and (d) excluding samples from the mid-Cretaceous of Myanmar. (e) Foreleg disparity in major mantispoid lineages through time, proxied by sum of variances, including samples from the mid-Cretaceous of Myanmar. The area around medians are 95% and 50% highest posterior density (HPD) intervals. Body size in major mantispoid lineages through time, proxied by the forewing length, (f) including samples from the mid-Cretaceous of Myanmar, and (g) excluding samples from the mid-Cretaceous of Myanmar. (h) Summary of maximum likelihood ancestral state reconstructions for body size on the partitioned time-calibrated tree.

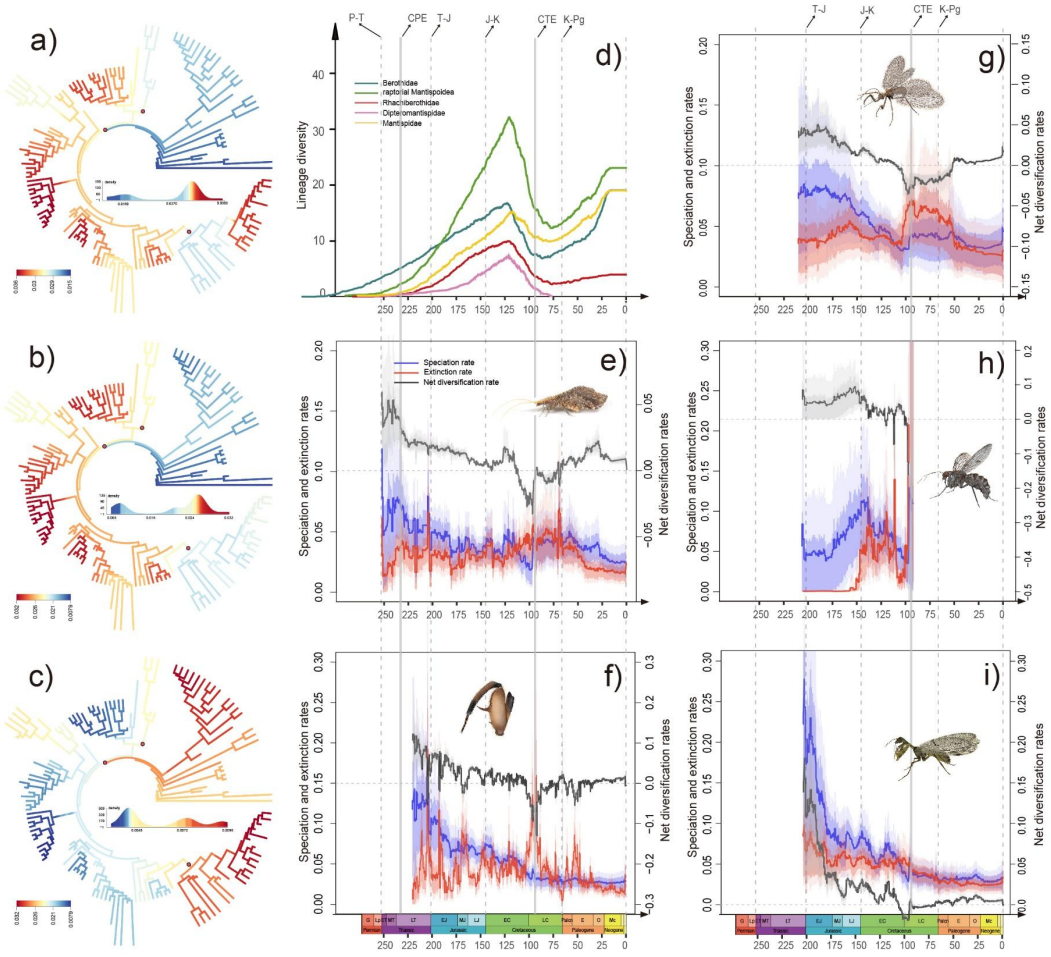

Figure 5. Diversification dynamics among major mantispoid lineages through time, including samples from the mid-Cretaceous of Myanmar. (a) Speciation rates, (b) Extinction rates and (c) Net diversification rates in partitioned time-calibrated trees, with corresponding rate density images, based on fossil-BAMM analysis. Red dots indicate the 95% credible rate shifts. (d) Lineage diversity through time, based on the birth-death information from the partitioned tip-dating Bayesian inference. Speciation rates, extinction rates and net diversification rates through time of (e) Berothidae, (f) Raptorial Mantispoidea, (g) Rhachiberothidae, (h) †Dipteromantispidae and (i) Mantispidae, estimated by MBD with the exponential model (-m 0 option), based on the

speciation and extinction information from the partitioned tip-dating Bayesian inference. The area around medians are 95% and 50% highest posterior density (HPD) intervals. Abbreviations: CPE, Carnian Pluvial Episode; CTE, Cenomanian-Turonian extinction event; J, Jurassic; K, Cretaceous; P, Permian; Pg, Paleogene; T, Triassic.

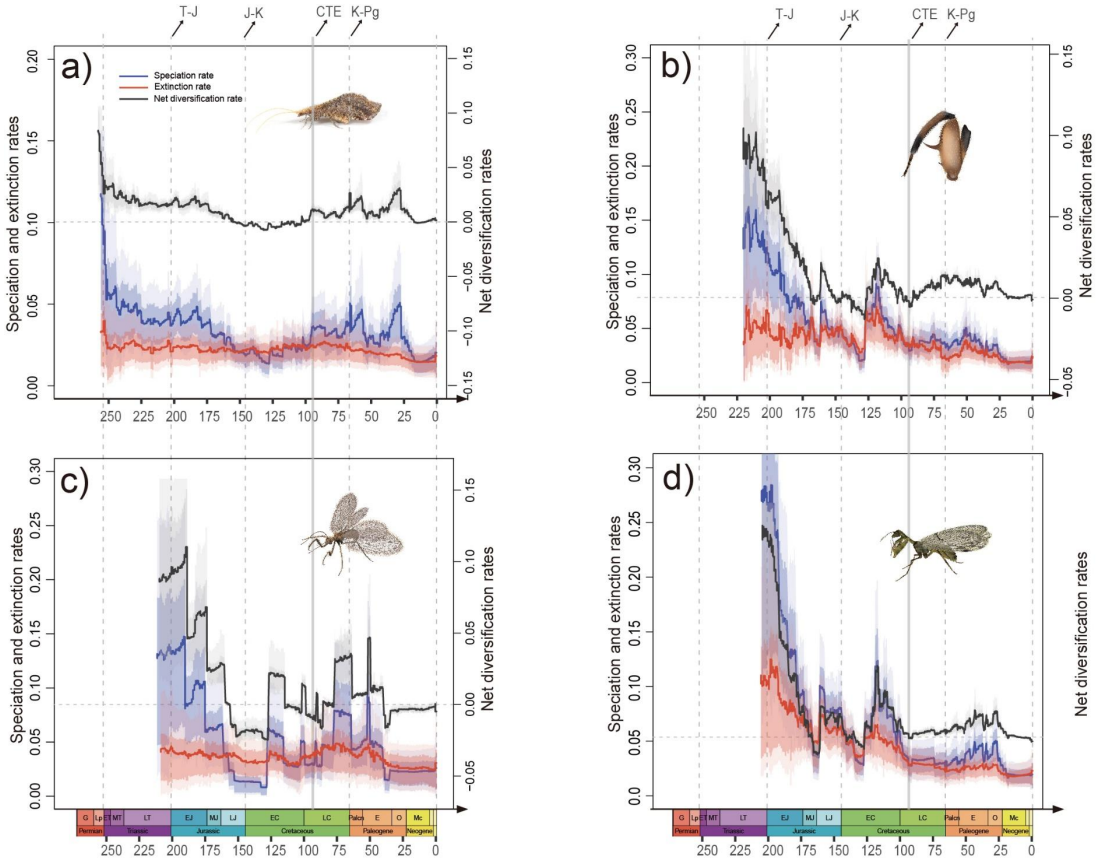

Figure 6. Diversification dynamics among major mantispoid lineages through time, excluding samples from the mid-Cretaceous of Myanmar. Speciation rates, extinction rates and net diversification rates through time of (a) Berothidae, (b) Raptorial Mantispoidea, (c) Rhachiberothidae and (d) Mantispidae, estimated by MBD with the exponential model (-m 0 option), based on the speciation and extinction information from the partitioned tip-dating Bayesian inference. The area around medians are 95% and 50% highest posterior density (HPD) intervals. Abbreviations: CPE, Carnian Pluvial Episode; CTE, Cenomanian-Turonian extinction event; J, Jurassic; K, Cretaceous; P, Permian; Pg, Paleogene; T, Triassic.

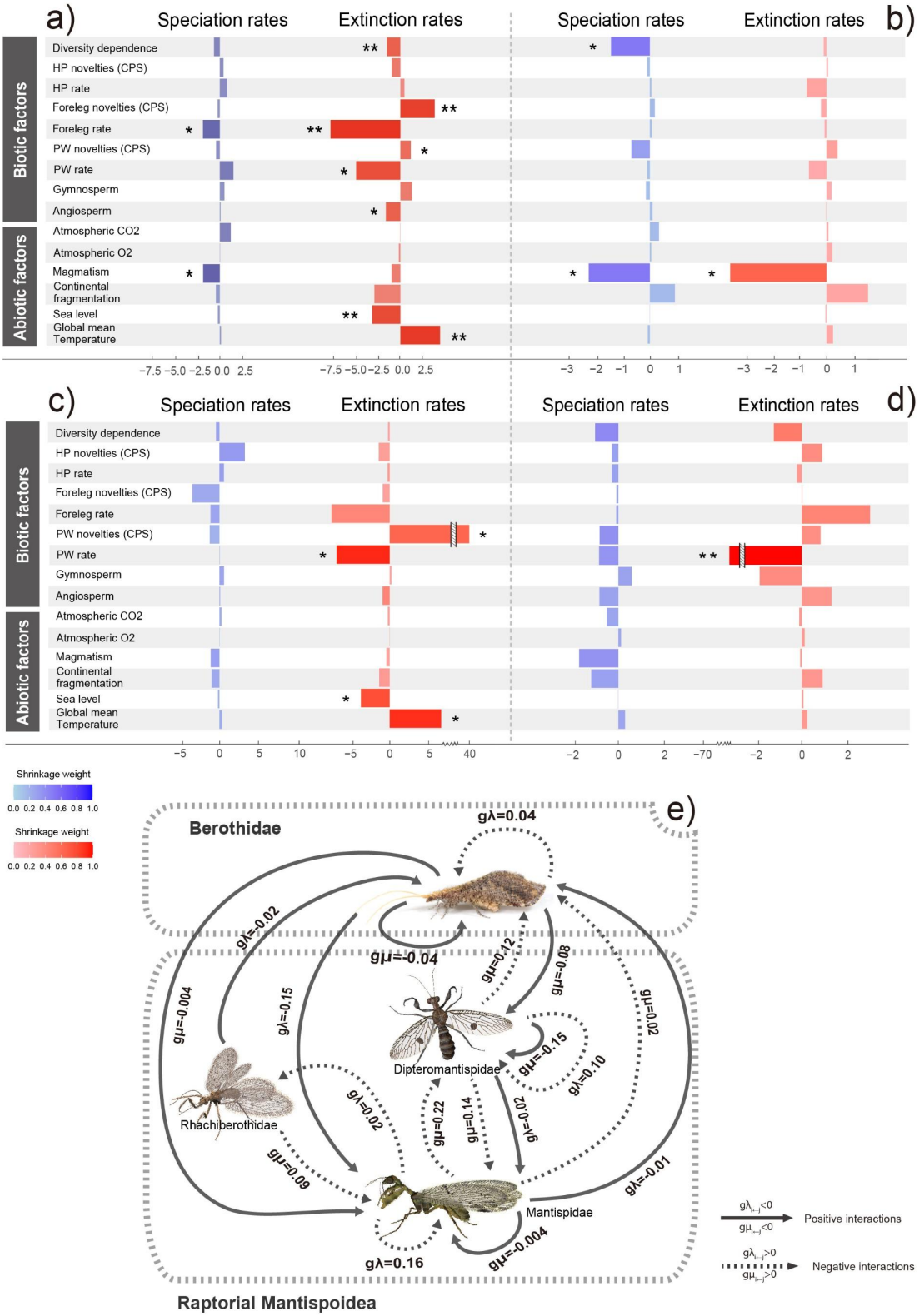

Figure 7. Bayesian inferences for paleoenvironmental and intrinsic correlation parameters on speciation and extinction, and for inter- and intraclade action within Mantispoidea, using the exponential model (-m 0 option). The paleoenvironmental and intrinsic correlation parameters on speciation and extinction of (a) overall Mantispoidea, (b) Berothidae, (c) Raptorial Mantispoidea and (d) †Dipteromantispidae, using the MBD model. One asterisk (*) indicates a weak support ($\omega < 0.5$) for a potential strong effect (95% HPD different from 0) or a strong

support (ω> 0.5) for a potential small effect (95% HPD crossing 0). Two asterisk (**) indicates a strong support for a potential strong effect (95% HPD different from 0). We did not directly conclude that the CPS value of PW correlates positively with extinction rate. Instead, we consider it to correlate negatively, because the proxy (CPS values) of PW generally increases (greater deviation) in a negative direction across time. Only the taxonomic groups with significant correlations are shown here, and others can be seen in Supplementary Figs. S120d, e S124, and Supplementary Table S9. (e) Network showing the diversity-dependent effects within and between clades on speciation and extinction rates (only significant correlations are shown, Table S10), using the MCDD model. Each arrow indicates the type of interaction imposed by a given group over another, which quantifies the proportion of rate change (decrease/increase for speciation or extinction) associated with the addition of one species of the competing group.